UNIVERSITY OF OKLAHOMA

GRADUATE COLLEGE

COMPARISON OF THE PERIOD FINDING ALGORITHMS ON WHITE DWARF BINARIES IN THE ZWICKY TRANSIENT FACILITY (ZTF) DATA RELEASE 3

A THESIS

SUBMITTED TO THE GRADUATE FACULTY

in partial fulfillment of the requirements for the

Degree of

MASTER OF SCIENCE

By

ONDER CATMABACAK
Norman, Oklahoma
2023

COMPARISON OF THE PERIOD FINDING ALGORITHMS ON WHITE DWARF BINARIES IN THE ZWICKY TRANSIENT FACILITY (ZTF) DATA RELEASE 3

A THESIS APPROVED FOR THE
HOMER L. DODGE DEPARTMENT
OF PHYSICS AND ASTRONOMY

BY THE COMMITTEE CONSISTING OF

Dr. Mukremin KILIC, Chair

Dr. Nathan KAIB

Dr. Xinyu DAI

To my loving cats Willow, Marceline, Marlow and Granma...

Table of Contents

Abstract

Irregular time series arise in most ground-based astronomical surveys due to atmospheric effects, missing observations, and instrumental issues that create erratic time intervals among data points and reduce data quality. Determining the exact period of a system can therefore be a problem. Building a correct mathematical formulation is required to analyze the unevenly-sampled data and reveal the hidden period information. Parametric techniques assume that the observable data can be represented as a linear combination of trigonometric functions of time. The non-parametric methods, on the other hand, are not affected by the assumptions about the shape of the underlying signal, which helps identify non-sinusoidal behavior.

In this thesis, we mainly consider two notable methods. The Lomb-Scargle periodogram [Lomb(1976)], and [Scargle(1982)], developed from the Least-Squares Spectral Analysis [Vaníček(1969)], is a known parametric algorithm for analyzing irregularly sampled time series for periodic signals. Conditional Entropy [Graham et al.(2013a)], conversely, is an example of non-parametric approaches originating from the Shannon entropy [Cincotta et al.(1995)], which uses the information theory and phase-folds the data at each trial frequency and estimates the conditional entropy $H(m|\phi)$ of the data, where m is the magnitude, and ϕ is the phase of the signal. According to information theory, the period with the least entropy corresponds to the correct frequency of a stationary signal.

In this thesis, we compare these two methods and identify the approach

that provides a better representation for the period of White Dwarf binaries we selected from Zwicky Transient Facility Data Release 3 [Masci et al.(2019)] [Bellm et al.(2018)]. Lomb-Scargle Periodogram predicted periods of 7 sources and failed to find correct periods of 8 sources from [Burdge et al.(2020b)]. Additionally, out of 34 WD binaries from ZTF DR3, Lomb-Scargle found 33 of them correctly. Conditional Entropy periodogram, on the other hand, accurately predicted periods of all objects. We conclude that Conditional Entropy proves to be more powerful than the traditional methods for detecting periodicities in time series data.

Chapter 1

Introduction

1.1 White Dwarfs

Following the evolution of a Main Sequence star with a mass smaller than $\sim 8M_{\odot}$, the remnant core of the star becomes a white dwarf (WD), as a result of the balance between the electron degeneracy pressure and star's gravity. Single white dwarfs usually have no stable energy sources, yet, if the progenitor star is metal-poor, some hot white dwarfs with hydrogen (H) atmosphere might have residual H burning that contributes to the luminosity of the WD (up to 30%) during its evolution [Miller et al.(2013)]. The star eventually cools down by radiating its thermal energy over time and turns into a black dwarf. The cooling timescale of the WD is much longer than the age of the Universe (13.7 Gyr), which might indicate why there is no observed black dwarf, to the best of our current knowledge, in the literature. Cooling timescale is also useful to set age limits on globular and open clusters as well as disks and halo populations [Richer et al.(1997)] [Hansen et al.(2002)] [De Marchi et al.(2004)] [Kilic et al.(2012)] [Kilic et al.(2017)].

The Mass-Radius relation of WDs involves an inverse proportion, $R \sim M^{-\frac{1}{3}}$, radius gets smaller with increasing mass. The typical mass range for White dwarfs is from 0.15 $M_{\odot}$ to 1.35 $M_{\odot}$ [Kilic et al.(2007)] [Kepler et al.(2007)]. WDs have a mass limit since the electron degeneracy pressure can balance the gravitational collapse until a certain point, then the WD either collapses or explodes,

depending on its type. ONeMg WDs with a sufficiently high rotation most likely turn into Neutron stars through accretion-induced collapse [Piro et al.(2014)] [Schwab et al.(2015)] [Liu et al.(2018)], in which the neutron degeneracy pressure establishes the ultimate balance against gravity. Alternatively, when electron degeneracy pressure fails to resist gravitational collapse, an explosion (type-Ia supernova) might occur if the white dwarf has a slow rotating Carbon-Oxygen core [Lieb et al.(1987)] [Hillebrandt et al.(2000)]. That mass limit was mathematically derived first by [Stoner(1929)] [Stoner(1930)] (1.1 $M_{\odot}$), and then [Chandrasekhar(1931)] (0.91 $M_{\odot}$). However, Chandrasekhar's calculation was performed through the implementation of the polytropic index for the non-relativistic pressure expression of the degenerate electron gas, taken from [Fowler(1926)], into the hydrostatic equation for gravitational equilibrium in Eddington's book, "*The Internal Constitution of the Stars*" [Eddington(1940)], in which the mass limit diverges from the actual value of 1.44 $M_{\odot}$ [Nauenberg(2008)].

White dwarfs are fascinating stellar objects, containing various physical phenomena under extreme densities, which make them the subject of a wide variety of research topics, including but not limited to gravitational waves, dense matter studies, binary systems with WDs, and exoplanet exploration. As once Sir Artur S. Eddington said at the centenary celebration of the Royal Astronomical Society [Eddington(1922)];

"*Strange objects, which persist in showing a type of spectrum out of keeping with their luminosity, may ultimately teach us more than a host which radiates according to rule.*"

1.1.1 White Dwarf Binaries

Binary systems play a major role in understanding the evolution of stars and testing stellar theories since half of the known stars are in binary systems. A particular case of binary systems is eclipsing binaries (EBs) which show regular brightness variation as one star passes by another and eclipses it. Astronomers can thus determine the relative size and radius of an object by measuring how much light it blocks in light curves.

Eclipsing binaries are separated into three categories; Algol, Beta Lyrae, and W Ursae Majoris types binaries, each showing distinct light curve patterns [Bienias et al.(2021)]. Algol (beta Persei) was the first eclipsing binary observed in [Goodricke(1783)]. Observations showed that Algol-type stars are dimmed by one-third of average brightness, periodically. Companion in Algol type binaries is in spherical or slightly ellipsoidal shape and has almost constant brightness between eclipses [Catelan and Smith(2015)]. They may have an invisible secondary eclipse if the size difference is significant. On the other hand, a typical Beta Lyrae type binary has an ellipsoidal companion and it is hard to distinguish the beginning and end of eclipses due to fluctuating brightness [Catelan and Smith(2015)]. Unlike Algol types, a relatively smaller secondary eclipse may occur. The last type of eclipsing binaries is W Ursae Majoris [Catelan and Smith(2015)], where the binary components are closer. In this case, the companion is distorted significantly, more than the other two types of binaries, by the primary star.

The first WD, 40 Eridani B, was observed in a multiple star system by

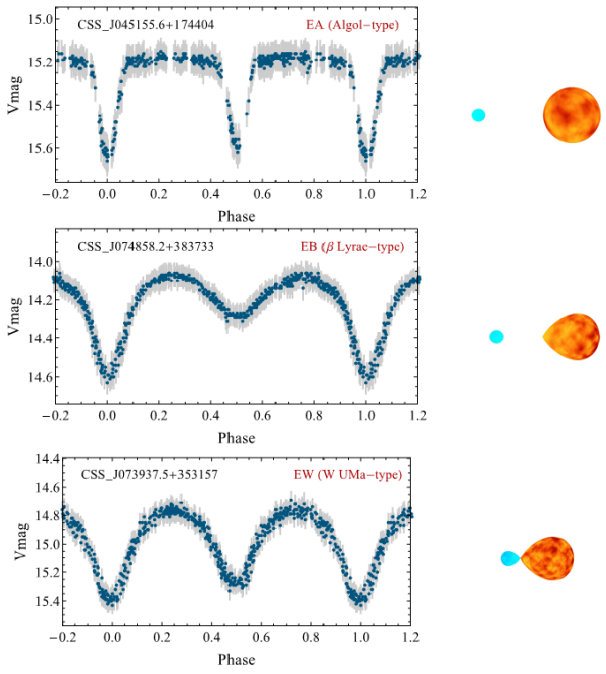

Figure 1.1: **Left:** Light curves for different eclipsing binary types. **Right:** Corresponding system configurations for EA (Algol type), EB (Beta Lyrae type) and EW (W Ursae Majoris type) binaries. Credit: [Fu et al. (2021)]

[Herschel(1785)] and was later confirmed by [Boss(1910)]. However, the first WD in an eclipsing binary, DQ Herculis 1934, was reported by [Wright(1935)]. The subsequent research focused more on short-period binaries [Marsh et al.(1995)] [Brown et al.(2010)][Kilic et al.(2010)] [Burdge et al.(2020b)] [Kosakowski et al.(2022)] as these systems are perfect examples to study binary evolution [Benz et al.(1990)] [Littlefair et al.(2008)] and gravitational waves [Burdge et al.(2019a)]. Correlation among eclipse timing variations(ETVs), eclipse duration variations(EDVs), and stellar radial velocities (RVs), may provide sufficient evidence for the detection of substellar companions around eclipsing binaries [Qian et al.(2012)] [Gong et al.(2018)] [Bellotti et al.(2020)].

1.2 General Properties of Irregular Time Series

The most basic definition of time series is given by a data set with a timestamp. There are many analysis techniques, the most well-known one is the Fourier Transform (FT) [Fourier(1822)]. Another method, Kalman filter [Kalman(1960)], is a prediction algorithm that makes forecasts about the future state of a system based on preceding estimations. Autoregressive-moving averages (ARMA), [Box and Jenkins(1970)], on the other hand, consist of two different polynomials. One of them reduces the time series into a single variable (moving averages) and the other makes predictions based on past data for regular time series [Scargle(1981)] [Feigelson et al.(2018)]. When a time series has uneven spacing between data points, however, time intervals vary significantly from each other in the series.

The nonlinearity in the data appears as a result of chaotic behaviors, where a system evolves from a deterministic to stochastic nature. [Scargle (1989b)] [Scargle(1990)] [Kulp(2013)].

In astronomical time series, the quality of a light curve depends on multiple factors. Noise, as one of them, is a series of uncorrelated random data points that have zero mean and constant variance. If the variables are independent and have zero means, the time series consists of white noise [Scargle(1989)]. In addition to the signal generated by the underlying process, one expects the time-series data to contain a white noise component [Scargle(1990)] [Scargle(1998)]. Therefore, the behavior of the analytical sequence can be assessed by the accurate description of a model, and based on the assumption that the irregular component is white noise, statistical inference can be used for the estimation [Scargle(1990)].

The ratio of the actual signal and the noise is called "Signal-to-Noise Ratio (SNR)", which provides and stipulates a quality measurement for the data. An acceptable ratio for astronomical detection should be at least five or more. One can find SNR in the measurement in terms of error as,

$$SNR = \frac{1}{e_m} \tag{1.1}$$

where e_m is the measurement error which should be 20% at most for SNR=5.

1.3 Periodogram

The periodogram is a signal processing technique in time series that allows one to find repeating patterns of regular or irregular frequencies, including periods and harmonics [Schuster(1898)] [Hernandez(1999)]. The periodogram is beneficial to time series such as the stock market's daily highs and lows, natural disasters including volcano eruptions, floods, and earthquakes, or the temporal variations in the spectra of stellar systems. There are various types of periodograms [Vityazev(1996)], and generally, a periodogram displays the significance of different frequencies and graphically shows how often specific frequencies appear in a time series. Although the method is different from the ordinary Fourier Transform of a signal, the periodogram gives an estimation for the Fourier Transform of the auto-correlation function (ACF), also known as power spectral density (PSD). The estimation provides an insight into how data points are related to each other and represents how power is distributed among different frequencies in a signal [Scargle(1981)] [Scargle(1982)]. If x(t) is a periodic signal,

$$x(t) = \sum_{n=-\infty}^{\infty} X_n e^{j2\pi \frac{n}{T} t} \tag{1.2}$$

then, for a given time T, the auto-correlation function of the periodic signal is,

$$R_x(\tau) = lim \frac{1}{2T} \int_{-T}^{T} x(t) x^*(t-\tau)\, dt \tag{1.3}$$

So, PSD can be written as,

$$PSD_x(f) = \mathcal{F}\{R_x(\tau)\} \tag{1.4}$$

where $\mathcal{F}\{R_x(\tau)\}$ is the Fourier Transform of the auto-correlation function $R_x(\tau)$. On the other hand, one can write the Schuster Periodogram [Schuster(1898)] as,

$$P_S(f) = \frac{1}{N}\left|\sum_{n=1}^{N} x(t_n)e^{-2\pi i f t_n}\right|^2 = |\mathcal{F}(x(t))|^2 \tag{1.5}$$

where N is the number of data points and f is the frequency that satisfies $0 \leq f \leq 1/t$. Even though Eq.1.5 shows that the Schuster periodogram equals the square modulus of Fourier Transform, unlike the Fourier analysis, periodogram analysis can directly transform the data into a PSD estimation. Furthermore, the Fourier transform processes a signal in the size of one window function at a time, whereas a periodogram examines an entire set of data points at once [Hernandez(1999)].

Due to the finite amount of data and infinite nature of the Fourier Transform, the power of a specific frequency in periodogram leaks to other frequencies and causes the misidentification of the frequency (aliasing or spectral leakage [Scargle(1982)]). This is a significant issue in signal processing, and the methods such as low-pass filters and improved sampling techniques would help decrease signal leakage.

All period-finding methods have the same restrictions for the range of detectable signals from the Nyquist–Shannon sampling theorem. According to the theorem, sampling should be greater than twice the maximum frequency in a

signal to preserve information and eliminate aliases. This specific frequency is called the Nyquist (folding) frequency. Finding this band-limiting frequency is an essential statistical condition for the efficient design of an experiment. In other words, it corresponds to the smallest periodicity available for the time series analysis [Vio et al.(2013)], [Vanderplas(2018)]. Periodograms are used for evaluating statistical significance without considering phase information [Vanderplas(2018)] [Hernandez(1999)].

When a periodogram is employed as a standard method for analyzing the light curves of stars, a folding process over many test periods, called phase folding, is applied to the data to find the frequency in a time series. First, the data is displayed according to the "phase" or on a binary scale concerning the trial period. The mean of the data is calculated at each phase interval, and the error is set to equal the variance in the interval. Epoch folding, on the other hand, is similar to period folding and uses phase but differs in starting point. While phase folding starts with the signal of any phase shifting, epoch folding takes off from a specific point that the observer can choose. Epoch folding calculates the maximum χ^2 over folding and the corresponding period is most likely period of the signal [Larsson(1996)]. Estimating detection significances has been a substantial focus on studies of the statistical features of epoch folding. [Schwarzenberg-Czerny(1989)].

Periodogram is not the best tool to analyze irregular time series but is functional. The simplicity of the periodogram's statistical behavior makes it worthwhile when evaluating the reliability of a possible detection [Scargle(1982)]. The more statistical investigation related to the subject can be found in [Scargle(1989)], and

see [Scargle(1998)][Scargle(2002)] for Bayesian blocks and estimation.

1.4 Period Finding Models in the Literature

The pursuit of precise frequencies in astrophysical events needs rigorous statistical data analysis. The periodogram is one of the most well-known methods due to its ease of use and widespread availability of efficient associated software. However, the use of periodograms in astronomical applications is not straightforward. Furthermore, in the event of irregular sampling, the ability to properly fix the statistical features of a periodogram is limited.

Next, we will summarize the pioneering works in the literature. As a result of rigorous research conducted in the past century, period-finding algorithms have changed significantly. "*Periodogram* was not built in a day", as the saying goes.

1.4.1 Schuster Periodogram

Arthur Schuster, [Schuster(1898)], is the founder of the mathematical approach to the period finding methodology, and he coined the name "periodogram" to describe it. It is hardly surprising that such a method was created in geophysics rather than astronomy since geophysical events are easier to observe, and seasonal characteristics in time series are critical in terms of the feasibility of observational studies in the discipline [Schuster(1898)].

Calculation of Schuster periodogram is based on a suspected periodicity, p. If one divides a time series on p, which is the first mathematical expression of phase folding, the resulting shape is [Schuster(1898)];

$$\begin{pmatrix} t_1 & t_2 & \dots & t_p \\ t_{p+1} & t_{p+2} & \dots & t_{2p} \\ \vdots & \vdots & \ddots & \vdots \\ t_{qp+1} & t_{qp+2} & \dots & t_{(q+1)p} \end{pmatrix}.$$

The sum of each rows are,

$$\begin{aligned} t_1 + t_2 + ... + t_p &= T_1 \\ t_{p+1} + t_{p+2} + ... + t_{2p} &= T_2 \\ &\vdots \\ t_{qp+1} + t_{qp+2} + ... + t_{(q+1)p} &= T_p \end{aligned} \tag{1.6}$$

Horizontal lines from the time series matrices can be represented , according to the [Schuster(1898)] using periodic series.

$$\begin{aligned} S = a_0 + a_1 cos(\theta) + a_2 cos(2\theta) + ... + a_p cos(p\theta) \\ + b_1 sin(\theta) + b_2 sin(2\theta) + ... + b_p sin(p\theta) \end{aligned} \tag{1.7}$$

where $\theta = 2\pi q/p$.

$$\begin{aligned} pa_0 &= T_1 + T_2 + ... + T_p \\ pa_1 &= 2[T_1 cos(\theta) + T_2 cos(2\theta) + ... + T_p cos(p\theta)] \\ pa_2 &= 2[T_1 sin(\theta) + T_2 sin(2\theta) + ... + T_p sin(p\theta)] \end{aligned} \tag{1.8}$$

If the periodicity that corresponds to the p intervals is obvious, then one should expect [Schuster(1898)],

$$\rho = \frac{r_1}{a_0}, \tag{1.9}$$

where $r_1 = \sqrt{a_1^2 + b_1^2}$.

$$\begin{aligned}\frac{\rho^2}{4} &= \frac{r_1^2}{4a_0^2} \\ &= \frac{(pa_1)^2 + (pb_1)^2}{4(pa_0)^2} \\ &= \frac{(T_1 cos(\theta) + T_2 cos(2\theta) + ... + T_p cos(p\theta))^2 + (T_1 sin(\theta) + T_2 sin(2\theta) + ... + T_p sin(p\theta))^2}{(T_1 + T_2 + ... + T_p)^2}\end{aligned} \tag{1.10}$$

gives an equation for periodicity. For T equals,

$$T = \frac{1}{a}\int_{t_1}^{t_1+T} f(t)cos(kt)dt + \frac{1}{b}\int_{t_1}^{t_1+T} f(t)sin(kt)dt \tag{1.11}$$

If one chooses T as multiple of $\frac{2\pi}{k}$, area under the curve $(\frac{2\pi}{k}, \sqrt{a^2 + b^2})$ stands for "periodogram of $f(t)$".

The Discrete Fourier Transform (DFT) and the Schuster periodogram are valuable tools for assessing power spectra when data are evenly separated in time [Vityazev(1996)]. Schuster Periodogram, as opposed to DFT, utilizes the notion of

PSD estimation for the signal and identifies the hidden periods in non-equispaced time series.

$$\hat{S}_p(f) = \frac{1}{N}\left|\sum_{j=0}^{N-1} x_j\, e^{-2\pi i f t}\right|^2 \tag{1.12}$$

Here the length of the time series is N, and x is the observation of a set of known and discrete periods. When the correlation coefficient reaches its maximum value, it equals the square of the normalizing factor's upper limit. As a result, the definitions of Least-Squares Spectra and Schuster periodograms diverge. [Vityazev(1996)].

One disadvantage of the Schuster periodogram is that the periodogram is suitable for small data sets and the algorithm becomes computationally expensive with the increasing number of samples. Furthermore, the smoothing process is done over time instead of frequency which causes resolution loss in the time domain.

1.4.2 Least-squares spectral analysis (LSSA)

According to [Vaníček(1969)], the least-squares spectral analysis (LSSA) is an approximate method of spectral analysis. The algorithm sometimes called the Vanicek method, is derived by averaging a generalized trigonometric function with unknown frequencies and coefficients over a mean-quadratic approximation. From the calculations of [Vaníček(1969)], the expression for the trigonometric polynomial T can be written as,

$$\begin{aligned} \overset{m}{T}(t) &= \sum_{j=1}^{m-1}(a_{0j} + r_j cos(w_j t - \phi_j)) \\ &= \sum_{j=1}^{m-1} T_j(t) \end{aligned} \tag{1.13}$$

where ω is frequency, and ϕ is the phase shift. It is reasonable to express $T_i(t)$ in terms of trigonometric functions such as,

$$T_j(t) = a_{0j} + a_j cos(\omega_j t) + b_j sin(\omega_j t) \tag{1.14}$$

$$a_{01} = \frac{1}{n}((t) - a_1 \sum cos(\omega_1 t)) = \frac{1}{n}(\sum F - a_1 Q) \tag{1.15}$$

where F is defined as a function of time for which one finds the period and

$$\begin{aligned} a_1 &= \frac{n\sum F(t)cos(\omega_1 t) - \sum F(t)cos(\omega_1 t)}{n\sum cos^2(\omega_1 t) - (\sum cos(\omega_1 t))^2} \\ &= \frac{n\sum F cos(\omega_1 t) - Q\sum F}{nQ_1 - Q^2} \end{aligned} \tag{1.16}$$

$$b_1 = \frac{\sum F(t)sin(\omega_1 t)}{\sum sin(\omega_1 t)^2} = \sum \frac{F sin(\omega_1 t)}{Q_2} \tag{1.17}$$

where $Q_2 > 0$ and Schwarz inequaltiy indicates $nQ_1 - Q^2 > 0$.

F can be converted into frequency space by using the mean-quadratic distance ρ as,

$$\begin{aligned} \rho^2 &= \sum (F(t) - T_1^*(t))^2 \\ &= \sum F^2 - a_{01}\sum F - a_1 \sum F cos(\omega_1 t) - b_1 \sum F sin(\omega_1 t) \end{aligned} \tag{1.18}$$

From here, one can define the least-square periodogram to show the dominant peak in a time series.

$$\sigma = \sum F^2 - \rho^2 \tag{1.19}$$

The least-square periodogram has a more robust power of differentiation for lower frequencies than the power spectrum, according to [Vaníček(1969)]. The LSS minima provide the most likely non-linear parameter combination. If the model is described correctly, the global LSS minimum should provide just the set of parameter estimates sought. As a result, the issue is reduced to the solution of LSS global minima. The least-square periodogram makes lower frequencies more easily distinguished than the power spectral density. However, computational cost increases as the mean-quadratic distance gets more complex.

1.4.3 Phase Dispersion Minimization (PDM)

Phase Dispersion Minimization (PDM), [Stellingwerf(1978)], is a non-parametric approach to search for non-sinusoidal pulsations that aim to reduce data dispersion while keeping the phase constant. It simultaneously produces the optimal least-squares light curve and period, which work well on irregularly spaced data and match well with highly non-sinusoidal temporal variations.

This approach is technically equivalent to the least-squares fitting, but the fit is closer to the mean curve determined through each bin rather than a fit to a specific curve (such as a Fourier component).

Let the variance of data be,

$$\sigma^2 = \frac{\sum (x_i - \bar{x})^2}{N - 1} \tag{1.20}$$

where x_i is the i^{th} data point, $\bar{x}$ is the average of data and N is the number of data points. Overall variance is given by,

$$s^2 = \frac{\sum(n_j - 1)s_j^2}{\sum n_j - M} \tag{1.21}$$

where M is the number of distinct samples. The ratio of two different variances above gives the statistics;

$$\Theta = \frac{s^2}{\sigma^2} \tag{1.22}$$

where Θ is the test statistic of the F-test. It reaches a local minimum for the trial period where the period is false when $\Theta \approx 1$ and true for $\Theta \approx 0$. The goal is to reduce the variance of the mean light curve, and no trigonometric functions are required. The method in [Stellingwerf(1978)] is subject to F-distribution. The PDM method, on the other hand, has greater pulse detection significance in the χ^2-distribution than the F-distribution (see Fig-2 in [Schwarzenberg-Czerny(1997)]). The reason is that the χ^2 distribution is a right-skewed and non-parametric distribution defined by degrees of freedom. The distribution approximates Gaussian with increasing degrees of freedom. Similar to the χ^2 distribution, the F-distribution is also skewed right, but it is a parametric distribution that assumes the data strictly obeys Gaussian distribution and is defined by two degrees of freedom with two different variables. In that sense, the χ^2 distribution seems to be a better fit for astronomical data sets since degrees of freedom are the same, and data do not have to follow the Gaussian distribution exactly.

1.4.4 Analysis of Variance (ANOVA)

In the analysis of variance (AOV) approach, [Schwarzenberg-Czerny(1996)], the data are fitted with periodic orthogonal polynomials, and the fit is evaluated according to how satisfactorily it fits the data. The parametric methods such as LSSA [Vaníček(1969)], Lomb-Scargle [Lomb(1976)], and [Scargle(1982)] make certain assumptions to characterize data in terms of trigonometric functions and employ poor statistical methods that do not meet expectations when finding the correct period of an irregular time series. A Fourier series with N harmonics is given by [Schwarzenberg-Czerny(1996)],

$$F^{(N)}(t) = \sum_{n=0}^{N} (a_n cos(n\omega t) + b_n sin(n\omega t)). \tag{1.23}$$

Observation X is formed as a result of the combination of the signal, F, and the noise, E, therefore variance in observation is written as [Schwarzenberg-Czerny(1996)],

$$(K-1)\widehat{Var}\{X\} = 2N \times \widehat{Var}\{F\} + (K-2N-1)\widehat{Var}\{E\} \tag{1.24}$$

where K is the number of data points. The ANOVA statistic defined as,

$$\begin{aligned} \Theta &= \frac{\widehat{Var}\{F\}}{\widehat{Var}\{E\}} \\ &= \frac{K-1}{2N}\left[\frac{\widehat{Var}\{X\}}{\widehat{Var}\{E\}} - 1\right] + 1 \end{aligned} \tag{1.25}$$

and is given in terms of frequency as,

$$\Theta(\omega) = \frac{(K-2N-1)(2N+1)\widehat{Var}\{F^{\{N\}}\}}{2N[(K-1)\widehat{Var}\{X\} - (2N+1)\widehat{Var}\{F^{\{N\}}\}]}. \tag{1.26}$$

The method uses the H_0 hypothesis, which means that the observation is completely white noise, [Neyman and Pearson(1928)], to determine the probability distribution of the periodogram.

Among the statistical advantages of the new period searching approach, there are adjustable and flexible Fourier modeling of oscillations, orthogonality, and the optimal AOV test that assures the highest sensitivity. The ANOVA statistics also avoid aliasing difficulties and provide a high SNR [Schwarzenberg-Czerny(1996)].

1.4.5 Lomb-Scargle Periodogram

The Lomb-Scargle periodogram ([Lomb(1976)] [Scargle(1982)]) is one of the most well-known methods for finding periodicity in non-uniformly collected time series. The periodogram peak is an essential feature to consider when a Lomb-Scargle periodogram will be used to determine whether a signal has a periodic component or not. The periodogram formula was proposed to detect the periodic sinusoidal signals in time series data, [Scargle(1982)], in the form,

$$P_{LS}(f) = \frac{1}{2}\left(\frac{(\sum_{i=1}^{N} x_i \, cos\omega(t_i - \tau_{LS}))^2}{\sum_{i=1}^{N} cos^2\omega(t_i - \tau_{LS}))} + \frac{(\sum_{i=1}^{N} x_i \, sin\omega(t_i - \tau_{LS}))^2}{\sum_{i=1}^{N} sin^2\omega(t_i - \tau_{LS})}\right) \tag{1.27}$$

where τ ensures the time shift-invariance for each frequency, and is given by;

$$\tau = \frac{1}{4\pi f} tan^{-1}\left(\frac{\sum_i sin(4\pi f t_i)}{\sum_i cos(4\pi f t_i)}\right) \tag{1.28}$$

[Lomb(1976)] evaluated the reliability and effectiveness of detection in the case of unevenly sampled data by utilizing the most widely used technique, the periodogram. A modification of the classical definition of the periodogram, [Schuster(1898)], was required to keep the specific statistical behavior of irregularly spaced data. In the limit of equidistant observations, [Scargle(1982)] found a formula for the transform coefficients similar to the ones found with the Discrete Fourier Transform (DFT). The DFT is virtually the same as the traditional periodogram method, but it is permitted for use with unequally spaced samples. The typical Lomb-Scargle periodogram is comparable to trigonometric functions in approximating the data at each frequency, as shown in Eq.1.28; with a possible extension toward a truncated Fourier series with multiple frequencies.

There is a reasonable chance, even with a low SNR, for an observed spectrum to match with the noise-free spectrum [Lomb(1976)]. The reason is that over a wide range of different frequencies, the noise in a signal will have a characteristic signature that helps us to identify and remove it from the signal. Because of the relation between noise and frequencies, noise has less impact on a spectrum than expected. If an observed spectrum and a noise-free spectrum of period p have an acceptable match, then p is the actual period. The ideal statistical features of the periodogram, on the other hand, are lost when signals are sampled irregularly, which is a typical circumstance in astronomy [Vio et al.(2013)].

Although the Lomb-Scargle Periodogram delivers better results than DFT, there are issues with using the Lomb-Scargle method to look for periodicities. Even though it provides a solution for non-equispaced data, Lomb-Scargle also suffers from the same aliasing problem that other methods have experienced. [Schwarzenberg-Czerny(1996)] claims that power spectrum by [Lomb(1976)] and [Scargle(1982)] does not follow the theoretical χ^2 probability distribution in real applications.

Chapter 2

Information Theory and Time Series

Information theory is one of the most widely used mathematical toolkits to analyze time series that simultaneously exhibit both nonlinearity and stochasticity. In astrophysics, stochastic fluctuations and dynamical instabilities are two phenomena that generate new information, although the idea of information is not limited to these specific circumstances. Before applying the information theory to time series, we must discuss probability and the probability distribution function.

2.1 Probability

In astronomy, we are interested in the probability of two simultaneous and correlated variables: the brightness of an observed source and time. The apparent magnitude depends on the star's luminosity and distance. Assuming that the distance of the source is known, the luminosity is the only factor that determines the brightness. The radiation emitted by a star is affected by the variations in the surface area of the star. For example, pulsating variable stars like Cepheids, RR Lyrae, and Mira variables alter their luminosity via periodic expansions and contractions (pulsations) [Cox(1980)]. Additionally, the companion in eclipsing binaries screens the surface of the primary star, which could be partially visible depending on the observer's line of sight, and reduces the star's luminosity [Kallrath & Milone(2009)]. Other mechanisms, such as accretion and bursts, can modify the luminosity through piled-up mass and extremely luminous outbursts

[Pringle & Rees(1973)]. According to the Eddington limit, the maximum luminosity changes with the star's mass [Frank, King & Raine(2002)]. Primary stars in binary systems (semi-detached or contact) accumulate matter from their companions [Hartmann(2008)]. Explosions such as novae take place on the surface of the WDs in close binary systems. A more energetic explosion such as a supernova occurs as a result of either the re-ignition of nuclear fusion in white dwarfs and neutron stars or the gravitational collapse of main sequence stars of masses $\geq 9M_{\odot}$ [José(2016)].

These events can increase or decrease the luminosity by orders of magnitude. As a result, fluctuations in brightness appear in the time series. Therefore, for an exact moment in time, the probability of brightness change can be described by various statistical approaches depending on whether the two variables are independent or not.

2.1.1 Marginal Probability

The marginal probability is the probability that an event occurs given the outcomes of another random variable. For instance, P(A) is the marginal probability of event A, which equals the sum of the probability that all other events occur.

$$P(A = a_i) = p_i = \sum_j p_{ij} \tag{2.1}$$

2.1.2 Joint Probability

A joint probability describes the chance of two (or more) events coinciding. For instance, there are two independent events, A and B, and the likelihood of these two events that occur at the same time is,

$$P(A \cap B) = P(AB) = P(A) \times P(B) \tag{2.2}$$

2.1.3 Conditional Probability

In Section-2.1.1, we presented how marginal probability is related to the probability of the occurrences of unrelated events. Alternatively, joint probability represents the odds of coexisting events. In the case of two or more dependent events, however, the probability will be dissimilar to both marginal or joint probabilities. Particularly, conditional probability grants us the likelihood of the occurrence of event A if another event B has previously occurred. The premise is that whether or not previous events have occurred may impact the probability of an event. The term "conditional" delineates that when we are asked to compute this sort of probability, we will be provided with additional criteria, constraints, or other information. Hence, the probability of A for a given B has occurred is

$$P(A|B) = \frac{P(A \cap B)}{P(B)} \tag{2.3}$$

.

One may express the joint probability in terms of the marginal and conditional

probabilities as

$$P(A \cap B) = P(A|B)P(B) \tag{2.4}$$

.

We note that

$$P(A \cap B) = P(B \cap A) \tag{2.5}$$

,

which means that the chance of both events A and B happening is the same as the probability of both events B and A happening. As a result, the equality of conditional probabilities can be written as

$$P(A|B)P(B) = P(B|A)P(A) \tag{2.6}$$

.

This implies that Bayes' theorem is applicable for reversing or converting a conditional probability as follows:

$$P(A|B) = \frac{P(B|A)P(A)}{P(B)} \tag{2.7}$$

.

Suppose the likelihood of one event's result has no bearing on the probability of another event's occurrence. The conditional probabilities of two independent

variables can then be written as

$$P(A|B) = P(A) \tag{2.8}$$

and

$$P(B|A) = P(B) \tag{2.9}$$

.

If A and B are mutually exclusive, they cannot coincide. Therefore, the conditional probability of mutually exclusive occurrences is always zero:

$$P(A|B) = 0 \tag{2.10}$$

$$P(B|A) = 0 \tag{2.11}$$

2.2 Entropy in Information Theory

Despite being described as a heat-related thermodynamic function by Clausius, Boltzmann was the first to portray the entropy in thermodynamics to assess the number of microscopic ways to achieve a given macroscopic state. The idea of entropy inspired Claude Shannon to develop the mathematical theory of measuring stochastic information losses [Shannon(1948)]. Information theory uses the entropy measure to choose between a set of potential solutions with the largest amount of information and a set of possible solutions with the least entropy. The theory only considers the probability of observing a specific event, so the contained information is a sum of the underlying probability distribution:

$$H(X) = -\sum_{i=1}^{N} p_i log(p_i) \tag{2.12}$$

.

The method of computing the information for a random variable is referred to as "entropy". It is a measure of the average amount of information needed to describe an occurrence of a random variable chosen from a probability distribution.

Let's imagine a coin toss experiment. When one flips a coin, there are two possibilities: heads or tails. In Figure-2.1, the combination of probabilities is represented on the x-axis as [heads, tail]. When there is an equal chance to get heads or tails, the uncertainty (entropy) is maximum. If one uses a fixed coin, the entropy in coin toss will be minimum. The reason is that coin flip provides all the information in the system since one can only have tails for every try. That is the simple logic of having most information at the lowest entropy.

2.2.1 Shannon Entropy

One of the most essential measurements in information theory is Shannon entropy. Shannon proposed statistical entropy as a critical notion in information theory to assess the missing average information in an unexpected source. [Shannon(1948)] proposed the notion of information entropy, sometimes known as Shannon entropy. In a broader sense, entropy is a random quantity determined by probability and may be used to measure the information about an event [Ellerman(2022)].

This measure of average uncertainty is called "entropy," H, by Claude Shannon. Shannon's chosen unit of entropy is based on the uncertainty of a fair coin toss,

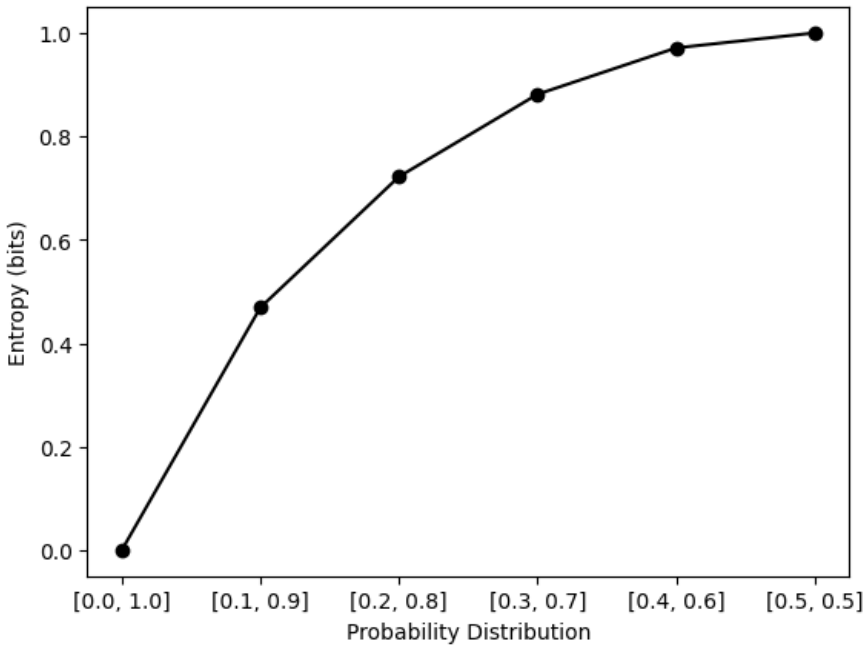

Figure 2.1: Correlation between information entropy and probability distribution. Uncertainty in system increases to right on x-axis.

which Claude Shannon refers to as a "bit." The bit is recognized as a unit of entropy because it represents the amount of information that is present [Shannon(1948)]. It measures the unpredictability of information. For example, we get either heads or tails when we flip a coin, with little or negligible probability of "edge." We know the collection of possible outcomes in that random experiment, but the actual outcome of a random experiment run is unknown. As a result, conveying one coin flip requires one bit of information, yet the outcome is uncertain. Whereby information is conserved in a closed system, a time series in our case, the most ordered combination of data is associated with the least entropy and the most information because Shannon's entropy measures the uncertainty of occurrences and eventually induces probability. The Venn diagram (Fig-2.2) displays the

relationships among various types of entropies.

2.2.2 Joint Entropy

The joint entropy, denoted as H(X, Y), where X and Y are random variables, measures the entropy in a combined system of two random variables. Depending on the logarithm base, we measure the joint entropy in bits. We can express the joint entropy as

$$H(X,Y) = -\sum_{i=1}^{N}\sum_{j=1}^{M} p(x_i, y_j) log(p(x_i, y_j)) \tag{2.13}$$

,

where the joint probability of random variables X and Y is $p(xi, yj)$. Although the marginal entropies of random variables X and Y are unequal, the joint entropy can be smaller than the sum of the marginal entropies. We therefore write

$$H(X,Y) \geq H(X) \tag{2.14}$$

$$H(X,Y) \geq H(Y) \tag{2.15}$$

$$H(X,Y) \leq H(X) + H(Y) \tag{2.16}$$

2.2.3 Mutual Information

When X and Y are random variables with joint entropy H(X,Y), the shared information between them is given as

$$I(X;Y) = H(X) + H(Y) - H(X,Y) \tag{2.17}$$

.

Here, one can confirm the mutual information's connection to the marginal and joint entropies for random variables X and Y. As we pointed out in the Eq-2.17, and like other entropies, mutual information is always positive. If we want to represent mutual information in terms of mutual probability,

$$I(X;Y) = -\sum_{i=1}^{N}\sum_{j=1}^{M} p(x_i, y_j) log(p(x_i; y_j)) \tag{2.18}$$

where we define the mutual probability as

$$p(x_i; y_j) = \frac{p(x_i, y_j)}{p(x_i)p(y_j)} \tag{2.19}$$

.

2.2.4 Conditional Entropy

We consider the case where one already knows the value of the second random variable, Y. We can calculate the entropy of the random variable X. We need to know the joint distribution of X and Y to compute the conditional entropy,

$$H(X|Y) = -\sum_{i=1}^{N}\sum_{j=1}^{M} p(x_i, y_j) log(p(x_i|y_j)) \tag{2.20}$$

,

where the conditional probability is written as

$$p(x_i|y_j) = \frac{p(x_i, y_j)}{p(y_j)} \tag{2.21}$$

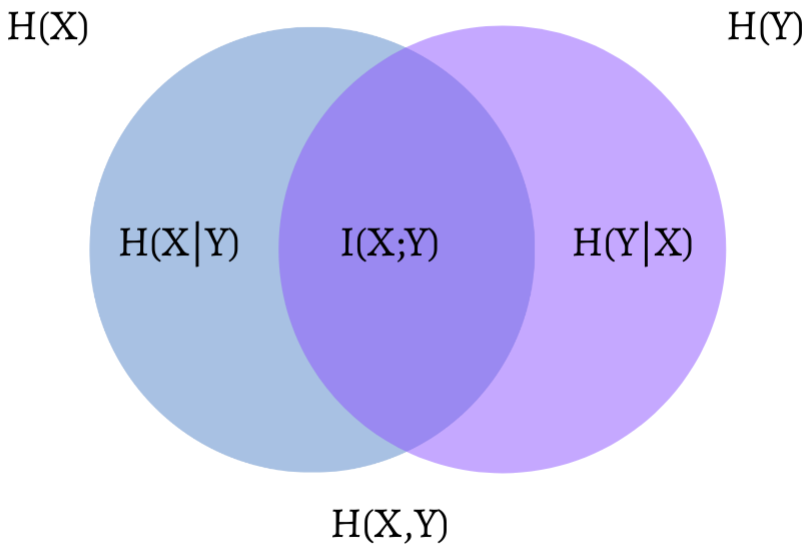

Figure 2.2: A Venn diagram illustrating the relation of X and Y. $H(X, Y)$ is the joint entropy. $H(X)$ and $H(Y)$ are the individual(marginal) entropies, $H(X|Y)$ and $H(Y|X)$ are the conditional entropies. $I(X; Y)$ is the mutual information.

.

Here, the conditional entropy can be expressed as a combination of joint and marginal probabilities,

$$H(X|Y) = H(X,Y) - H(Y) \tag{2.22}$$

.

It is worth noting that we only utilize the marginal entropy and probability with a known value for the random variable. All entropies have a relationship, which one can express in terms of mutual information as

$$H(X|Y) = H(X) - I(X;Y) = H(X) - I(Y;X) \tag{2.23}$$

.

2.3 Entropy-based Period Finding Methods

2.3.1 Conditional Entropy

A light curve is most typically represented using a least-squares fit to a series of trigonometric functions ([Lomb(1976)] and [Scargle(1982)]. There are also other attempts to minimize dispersion in phase space. For example, [Cincotta et al.(1995)] [Cincotta et al.(1999a)] and [Cincotta et al.(1999b)] presented a method where the Shannon entropy of the period of an irregular time series was minimized via folding the period by a test period. When data points are folded over the correct period, the light curve produces the most information about a signal. By minimizing the entropy of a system, one minimizes its informational deficit, and the theory of information can prove this to be mathematically correct.

[Graham et al.(2013a)] introduced a new method based on information theory, the conditional entropy (CE), of the light curve. The algorithm's foundation frequently dictates how effectively it can handle the most basic components of time series data. Fourier analysis cannot cope with irregularity in time series as much as entropy methods can. When detecting cycles and defining periodic behavior, conditional entropy is equivalent to Shannon and maximal entropy in evaluating synthetic data, but it outperforms them on actual data [Graham et al.(2013a)]. As [Graham et al.(2013a)] suggested this new method, conditional entropy, improves the results of the former entropy-based methods. [Graham et al.(2013a)] showed that conditional entropy can detect cycles in standard aggregate and time-series data.

Conditional entropy (CE), $H(m_i|\phi_j)$, is a constraint quantity that is defined as a combination of the joint probability of normalized magnitude and phase with the marginal probability of phase [Graham et al.(2013a)],

$$H(m_i|\phi_j) = \sum_{i,j} p(m_i, \phi_j) ln \left(\frac{p(\phi_j)}{p(m_i, \phi_j)} \right) \tag{2.24}$$

,

where the phase probability is,

$$p(\phi_j) = \sum_{i} p(m_i, \phi_j) \tag{2.25}$$

.

Most parametric methods for period-finding algorithms have a downside: period harmonics are misidentified as the correct period, a typical situation for binary systems. The actual peak in a periodogram may correspond to the harmonics of the correct period because, for eclipsing binaries, there are no statistical differences between the accurate period and its harmonics [Graham et al.(2013b)]. However, approaches seeking sinusoidal-like variations predict only one of these periods. In that sense, CE is the best algorithm for revealing periodic behaviors in both sinusoidal and non-sinusoidal signals [Graham et al.(2013b)].

Chapter 3

Light Curves from The Zwicky Transient Facility Data Release 3

The Zwicky Transient Facility (ZTF), named after Fritz Zwicky, was built as the successor of the Palomar Transient Factory (PTF) (2009-2012) [Rau et al.(2009)]. One of the purposes of the ZTF is to uncover the population of variable stars with periods less than a few hours in the Milkyway Galaxy [Graham et al.(2019)]. ZTF uses the upgraded 1.2 meters Samuel Oschin Telescope at Palomar Observatory to scan the Northern sky in optical bands (R-band and SDSS g') every two days [Bellm(2014)] [Bellm et al.(2018)]. Observations have 30 seconds exposure time, 10 seconds readout time, and 15 seconds time interval between exposures [Bellm(2014)].

3.1 Data and Period Finding

The data were chosen from the third data release of the Zwicky Transient Facility (ZTF DR3) [Bellm et al.(2018)] [Masci et al.(2019)]. The Lomb-Scargle and Conditional Entropy periodograms were used on data to plot light curves. For period finding techniques, we utilized particular packages from the `Python` programming language, such as `LombScargle` under `astropy.timeseries`[1] and conditional entropy algorithm from `cuvarbase`[2].

The analysis consists of two sections. First, I selected 15 sources from

[1]https://docs.astropy.org/en/stable/timeseries/lombscargle.html
[2]https://johnh2o2.github.io/cuvarbase/index.html

[Burdge et al.(2020b)] to test the Conditional Entropy algorithm. The recipe described in Appendix in [Burdge et al.(2020b)] was followed to produce light curves. Light curves generated with the Lomb-Scargle periodogram are also provided for these sources to compare them with the Conditional Entropy periodogram in section-3.3. Next, 34 WD binaries, with periods under 2 hours selected from ZTF DR3, are used as the main challenge between the Conditional Entropy and the Lomb-Scargle periodograms.

3.2 Testing Conditional Entropy periodogram

I tested the usefulness of the Conditional Entropy periodogram before making a comparison between the periodograms. The test includes finding periods of 15 WD binaries from [Burdge et al.(2020b)]. Conditional Entropy periodogram light curves plotted with signal parameters borrowed from [Burdge et al.(2020b)], described in Appendix-B. Typical period search includes approximately a couple of million iterations over trial frequency per source to find the best light curve. The best result is to have a light curve with the lowest conditional entropy. Test results are provided in this section and an actual comparison done between two periodograms is presented in the section-3.3.

ZTF J1539+5027 is an eclipsing double white dwarf binary with an ultra-short period (6.91 minutes), top left corner in Figure-3.1, first discovered by [Burdge et al.(2019a)] [Keller et al.(2022)]. The brighter star is a He-WD, ZTF J1539+5027 A, which is three times heavier than its companion ($M = 0.21 M_{\odot}$),

ZTF J1539+5027 B, and has half of its radius ($R = 0.00314R_{\odot}$). The system is also expected to be a strong source of gravitational waves due to the short orbital period. However, no X-ray flux is observed [Burdge et al.(2019a)]. There is also no evidence for continuous accretion, but the high surface temperature of the primary star ($\sim 50,000$ K) may indicate that intermittent accretion is still possible [Burdge et al.(2019a)]. Light curves from both periodogram algorithms, Figure-3.2, clearly show the correct period (6.91 minutes).

ZTF J0538+1953 is another eclipsing and detached double WD binary with 14.4 minutes period in Figure-3.1 [Burdge et al.(2019b)][Burdge et al.(2020b)]. The primary star is a $M = 0.45M_{\odot}$ He or CO WD while the companion is $M = 0.32M_{\odot}$ He WD. Lomb-Scargle and Conditional Entropy periodograms detected the period as 14.4 minutes in Figure-3.2.

ZTF J1905+3134 is a rare type of cataclysmic variable star, an eclipsing AM CVn. It has a short orbital period, 17.2 minutes (see Figure-3.1) [Burdge et al.(2020b)] [Keller et al.(2022)]. [Burdge et al.(2020b)] also states that accretion and eclipse are present. We do not have any mass or radius information about the system, due to the contribution of a high mass transfer rate to luminosity. Conditional Entropy periodogram obtained the correct period, 17.2 minutes, in Figure-3.2

PTF J0533+0209 is a double WD system that shows robust ellipsoidal modulation in lightcurve (Figure-3.1). The primary star is a $M = 0.65M_{\odot}$ CO-WD where the companion is a He-WD ($M < 0.2M_{\odot}$) with a helium-dominated atmosphere [Burdge et al.(2019b)]. [Burdge et al.(2019b)] states that the system is non-interacting. The conditional Entropy periodogram found that the orbital

period is 20.57 minutes. The Lomb-Scargle algorithm could not identify the correct period in Figure-3.3. On the other hand, a harmonic of the period, 10.28 minutes, is classified as the correct period.

ZTF J2029+1534 is another eclipsing double white dwarf binary, introduced in [Burdge et al.(2020b)]. The system consists of two He-WD with similar massses ($M_1 = 0.32M_\odot$ and $M_2 = 0.3M_\odot$) and the period is 20.9 minutes (Figure-3.1) [Burdge et al.(2020b)]. The Lomb-Scargle periodogram anticipated the light curve correctly, however, the Lomb-Scargle power indicates the founded period is incorrect. It also extracted half of the period as another potential period, again, false alarm probability excluded that option as well.

ZTF J0722-1839 is an eclipsing and interacting double He-WD binary with 23.7 minutes period (Figure-3.1) [Burdge et al.(2020b)]. Stars have similar masses ($M_1 = 0.38M_\odot$ and $M_2 = 0.33M_\odot$) as well as other features such as temperature, radius, and luminosity [Burdge et al.(2020b)]. Periodogram results are similar ones with ZTF J2029+1534, where the Lomb-Scargle periodogram failed again to identify powers in Figure-3.1. Light curves of the period and its harmonics, though, are accurately determined. False alarm probability implies that both light curves do not have statistical significance [Baluev(2007)].

ZTF J1749+0924 is most probably another eclipsing He-WD pair with 26.4 minutes orbital period (Figure-3.1) [Burdge et al.(2020b)]. The system shows some resemblance to ZTF J2029+1534, however, the mass gap between individual components of the system ($M_1 = 0.4M_\odot$ and $M_2 = 0.28M_\odot$) is distinct. Conditional Entropy managed to get a true period while Lomb-Scargle maintained

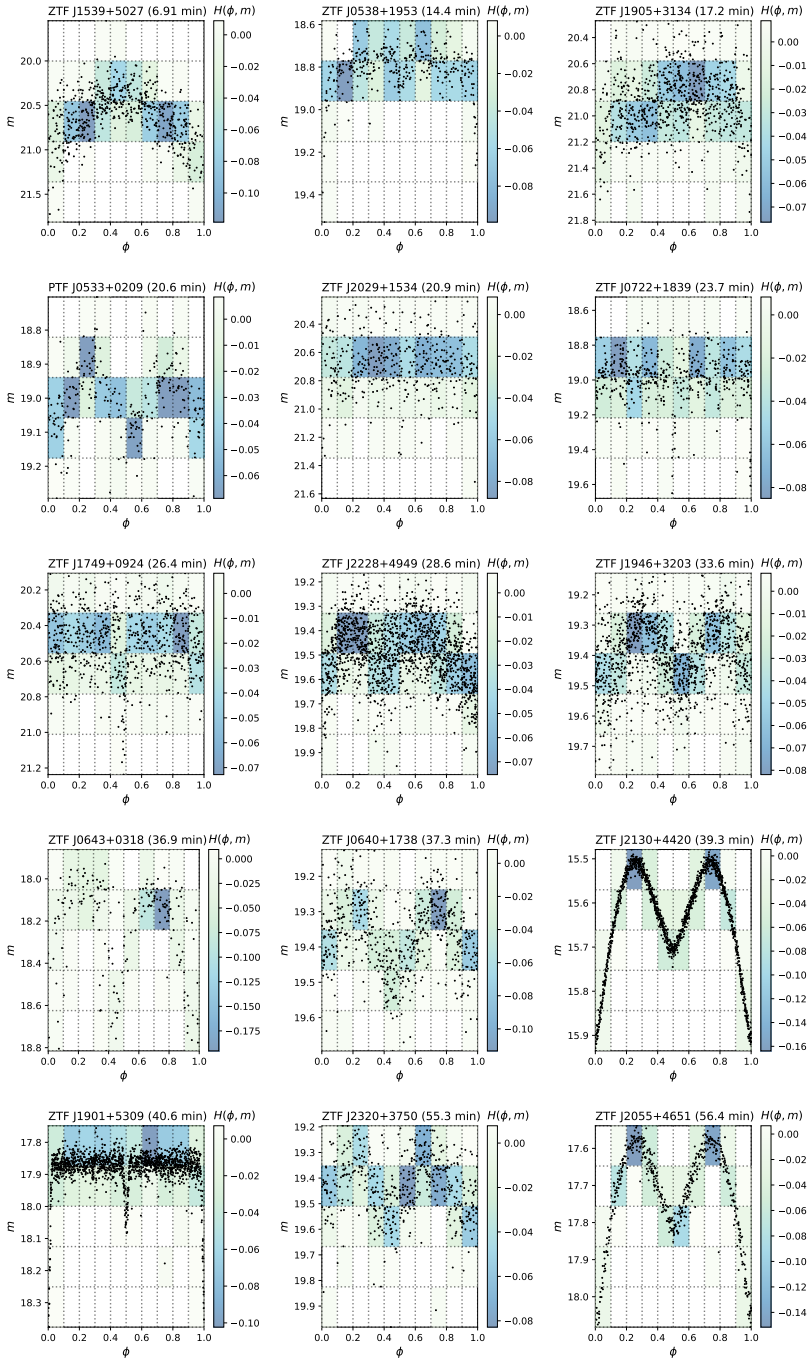

Figure 3.1: 15 sources from [Burdge et al.(2020b)] used for testing Conditional Entropy periodogram. The algorithm ensures that the minimum value of Conditional Entropy (f=argmin($H(\phi, m)$)) is selected.

Table 3.1: Binary WDs with a period under 60 minutes from [Burdge et al.(2020b)]. "E" means the system has eclipsed,

Source Name	RA-DEC (deg)	Type	P (min)
ZTF J1539+5027	234.88400 +50.46078	DWD+E	6.91
ZTF J0538+1953	84.51132 +19.88416	DWD+E	14.44
ZTF J1905+3134	286.29727 +31.57566	AM CVn +E	17.2
PTF J0533+0209	83.38358 +2.15325	DWD	20.57
ZTF J2029+1534	307.34286 +15.57525	DWD+E	20.87
ZTF J0722-1839	110.58951 -18.65846	DWD+E	23.7
ZTF J1749+0924	267.48038 +9.40906	DWD+E	26.43
ZTF J2228+4949	337.11273 +49.82125	AM CVn	28.56
ZTF J1946+3203	296.51617 +32.05363	WD+sdB+E	33.56
ZTF J0643+0318	100.90318 +3.30762	WD+E	36.91
ZTF J0640+1738	100.07788 +17.64585	WD+sdB	37.27
ZTF J2130+4420	322.73627 +44.34625	WD+sdB+E	39.34
ZTF J1901+5309	285.35593 +53.15818	DWD+E	40.6
ZTF J2320+3750	350.08524 +37.84188	DWD	55.25
ZTF J2055+4651	313.81656 +46.85178	WD+sdB+E	56.35

E: eclipsing, **WD**: white dwarf, **DWD**: double white dwarf, **sdB**: subdwarf B-type, **AM CVn**: AM Canum Venaticorum.

neither a clear light curve nor Lomb-Scargle power for both periods and its harmonics in Figure-3.1.

ZTF J2228+4949 shows characteristic features of an AM CVn system such as high accretion, and double-peaked He-II emission but no hydrogen line in spectra. The orbital period is 28.56 minutes (Figure-3.1) [Burdge et al.(2020b)]. There are no observational restrictions on AM CVn masses in the literature, except having high mass WDs, due to the contribution to luminosity from high mass accretion rate, similar to ZTF J1905+3134[Ramsay et al.(2018)]. Both algorithms computed the orbital period precisely as 28.6 minutes in Fgiure-3.2.

ZTF J1946+3203 is a He WD - sdB binary with similar masses ($M_1 = 0.27M_\odot$ and $M_2 = 0.3M_\odot$) [Burdge et al.(2020b)]. Despite having similar masses, the radii of components are quite different ($R_1 = 0.3R_\odot$ and $R_2 = 0.11R_\odot$) which is also the case for their temperatures ($T_1 = 11,500K$ and $T_2 = 28,000K$). The system shows an eclipse and the orbital period is 33.56 minutes [Burdge et al.(2020b)]. Conditional Entropy and Lomb-Scargle periodograms agree on the orbital period in Figure-3.2.

ZTF J0643+0318 is an interacting binary of He-WDs. The system has 36.91 minutes orbital period, seen in Figure-3.1 [Burdge et al.(2020b)]. Lomb-Scargle periodogram delivered a clear result of the orbital period in Figure-3.4. However, the period detection falls below the detection limit with a high false alarm probability [Baluev(2007)].

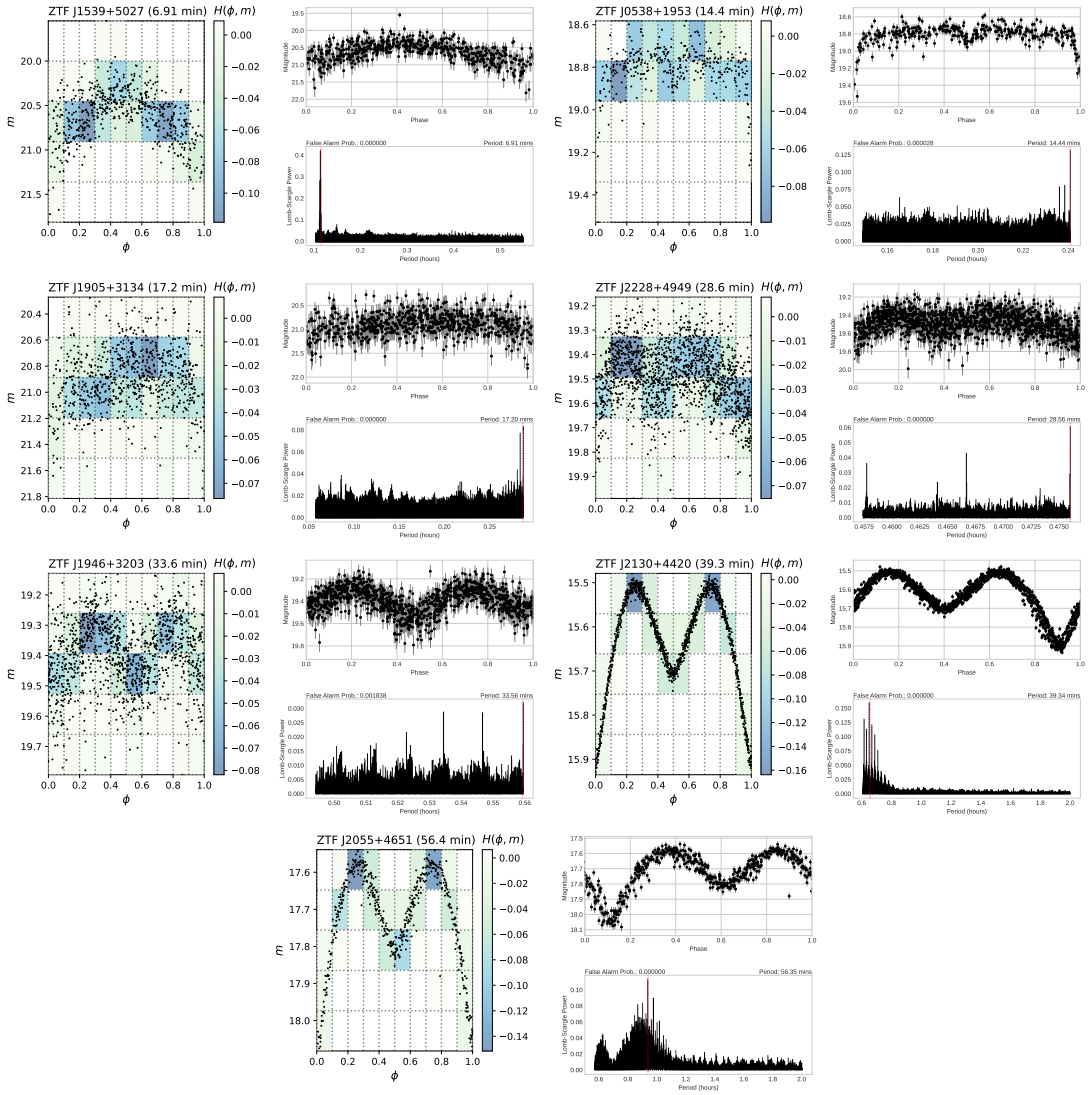

Figure 3.2: Lomb-Scargle periodogram testing for the sources in Figure-3.1 and comparison to results from Conditional Entropy periodogram. Both periodogram algorithms found the same period for the 7 sources in [Burdge et al.(2020b)].

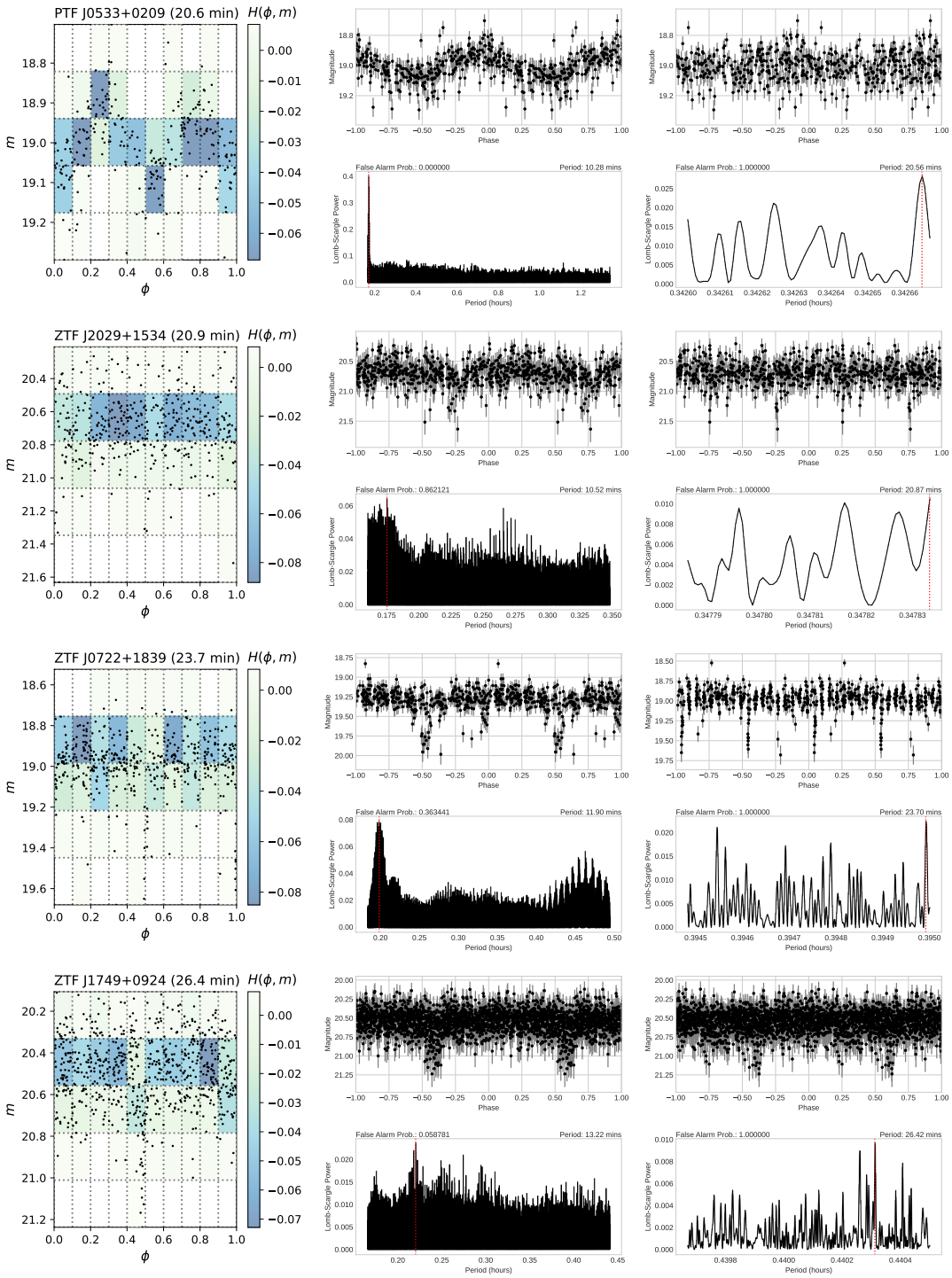

Figure 3.3: Lomb-Scargle periodogram testing for the sources in Figure-3.1 and comparison to results from Conditional Entropy periodogram. Conditional Entropy periodogram algorithms found the correct periods for 7 sources. However, the Lomb-Scargle periodogram identifies the correct orbital period as half of the orbital periods in the literature.

ZTF J0640+1738 is an ellipsoidal interacting binary, WD+sdB, (Figure-3.1) [Burdge et al.(2020b)]. The system has comparable compositions to ZTF J1946+3203. There is a small mass gap between companions ($M_1 = 0.39M_\odot$ and $M_2 = 0.325M_\odot$) and a significant surface temperature difference ($T_1 = 10,200K$ and $T_2 = 31,500K$), as well. The orbital period is 37.27 minutes [Burdge et al.(2020b)]. Lomb-Scargle periodogram found light curves for the correct period, and for half of the period, yet, false alarm probability failed to identify the correct period in Figure-3.4.

ZTF J2130+4420 is identified by [Kupfer et al.(2020)] as sdOB- CO-WD binary. It is also stated in [Kupfer et al.(2020)] that the companion ($0.337M_\odot$) filled the Roche lobe and is transferring matter onto WD with a mass of $0.545M_\odot$. In [Kupfer et al.(2020)] and [Burdge et al.(2020b)], the period is indicated as 39.34 minutes in Fig-3.1. The system is one of the brightest objects in this work, with 15.5 magnitudes. It also has eclipse and mass transfer between companions. [Rivera et al.(2019)] and [Ramsay et al.(2019)] suggest that the system is an AM CVn. The algorithms have no issue finding the correct period in Figure-3.4.

ZTF J1901+5309 is another eclipsing double WD system having an orbital period at 40.6 minutes in Figure-3.1) [Coughlin et al.(2020)] [Burdge et al.(2020b)]. Both stars have masses of $0.36M_\odot$, however, there are differences in radius ($R_1 = 0.03R_\odot$ and $R_2 = 0.022R_\odot$) and temperatures ($T_1 = 26,000K$ and $T_2 = 16,500K$). [Coughlin et al.(2020)] explains that the system is a detached binary. Light curves have no trouble finding the exact period of the system. False alarm probability, on the other hand, indicated a 45% chance that the correct

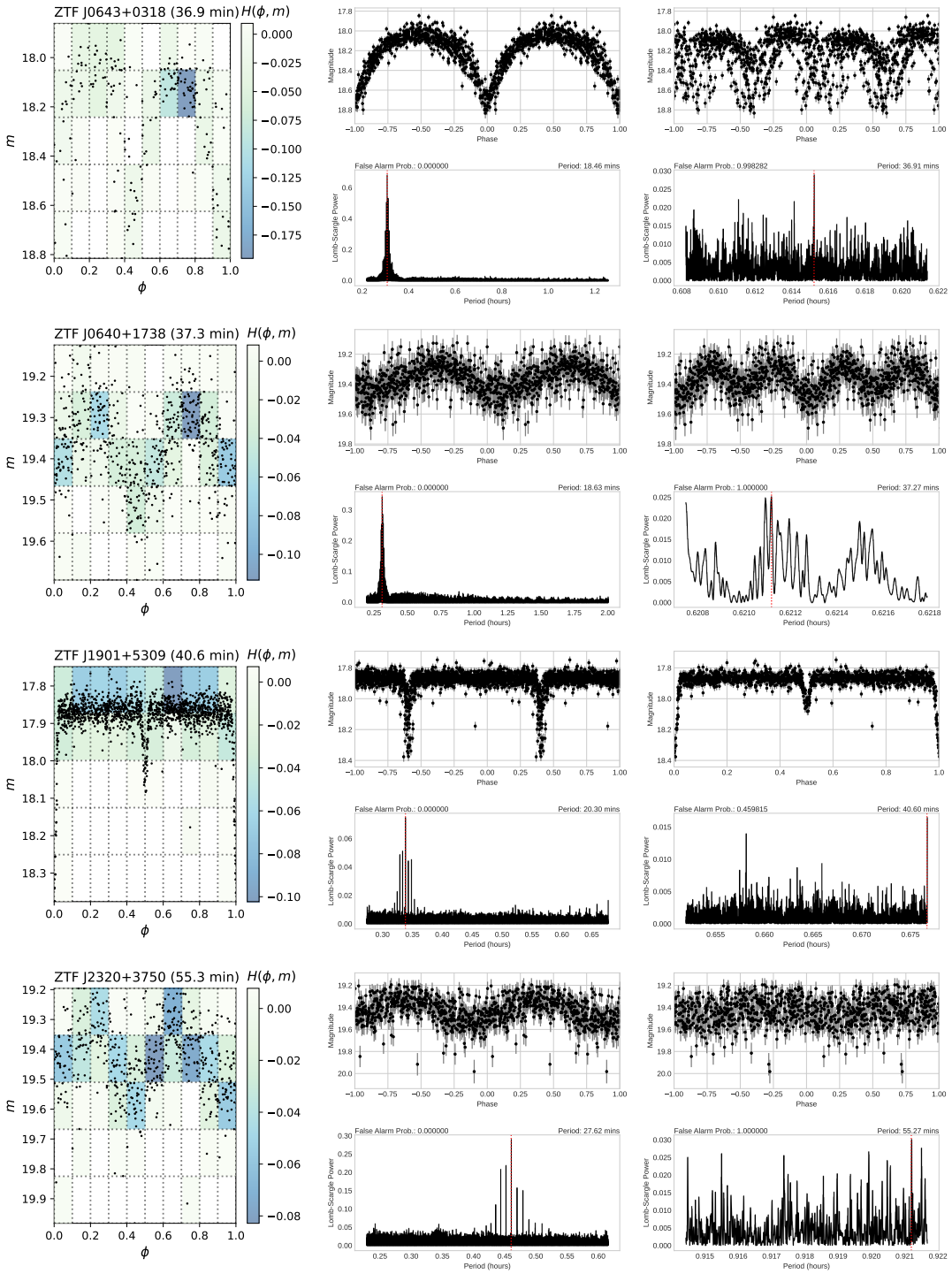

Figure 3.4: Continued from Figure-3.3.

period is false (see Figure-3.4).

ZTF J2320+3750 is the third rotating ellipsoidal variable, a double WD binary, in this section that a $0.2M_{\odot}$ He-WD revolves around $0.69M_{\odot}$ CO-WD with a 55.3 minutes orbital period in Fig-3.1 [Burdge et al.(2020b)]. ZTF J2320+3750 was falsely identified by the Lomb-Scargle periodogram with half of the correct period in Figure-3.4.

ZTF J2055+4651 is an Algol type He-sdOB+WD binary system, with a period of 56.35 minutes [Kupfer et al.(2020)] [Keller et al.(2022)] [Burdge et al.(2020b)]. There is ongoing mass transfer on a massive WD [Burdge et al.(2020b)]. Fig-3.1 exhibits that the Lomb-Scargle periodogram found the orbital period of the system, correctly (see Fig-3.2).

Figure-3.1 shows that one can acquire the exact results in [Burdge et al.(2020b)] with a Conditional Entropy periodogram. Hence the Conditional Entropy periodogram is a valid tool to generate light curves with correct orbital periods. Lomb-Scargle periodogram, on the other hand, found light curves of 7 sources correctly in Figure-3.2. The remaining 6 sources in Figure-3.3 and Figure-3.4 were misidentified by the Lomb-Scargle periodogram. The other 2 sources, ZTF J0640+1738 and ZTF J1901+5309 in Figure-3.4, have the correct period, but their false alarm probabilities are above the allowed limit, $\leq 10\%$.

3.3 White Dwarf Binaries in ZTF DR3

I analyzed 10,117 lightcurves in the data set (8529 r-band, 1101 g-band, and 487 i-band), in which 282 sources have an orbital period under 2 hours. I selected 34 sources, out of these 282 sources, with at least one WD component, presented in Tables 3.2-3.3-3.4. 10 of these sources have an orbital period under 90 minutes, 12 of them are between 90-100 minutes, and 12 sources have a period between 100-120 minutes. I applied Conditional Entropy and Lomb-Scargle periodograms to 34 sources and compared the light curves.

ZTF J2243+5242 is an Algol type eclipsing double WD binary with an ultra-short orbital period (8.8 minutes) [Burdge et al.(2020a)]. Components of the system have similar masses ($M_1 = 0.35M_\odot$ and $M_2 = 0.38M_\odot$), radius ($R_1 = 0.0308R_\odot$ and $R_2 = 0.0291R_\odot$), and effective surface temperatures ($T_1 = 22,200K$ and $T_2 = 16,200K$) [Burdge et al.(2020a)]. Lomb-Scargle and Conditional Entropy periodograms plotted light curves, seen in Figure-3.5. The Conditional Entropy method provides a clear light curve that shows the correct period where the Lomb-Scargle failed to obtain the period.

ZTF J1851+1714, also known as ZTF18abnbzvx, is a highly magnetized, rapidly rotating white dwarf pulsar (WDP) candidate at a period of 12.37 minutes [Kato & Kojiguchi(2021)]. The source has large amplitude change with an ultra-short period but no eclipse or mass transfer is recorded [Kato & Kojiguchi(2021)]. It is also stated that the source emits X-rays[3]. There is no mass information in

[3]https://www.astronomerstelegram.org/?read=14973

the literature. Light curves generated from both periodograms are consistent in that the period is 12.37 minutes (Figure-3.5).

ZTF18aaplouo (Gaia14aae) is first discovered by William Herschel Telescope in 2014 [Rixon et al.(2014)]. Characterization of a deeply eclipsing AM CVn-system is also described in [Campbell et al.(2015)] and [Marcano et al (2021)]. White Dwarf of the system has at least $0.78 M\odot$ and accretes mass from 0.015 M$\odot$ companions and regularly exhibits outbursts [Campbell et al.(2015)] [Marcano et al (2021)]. Both periodograms have found light curves with a $\sim$ 3 magnitude deep eclipse at a period of 49.7 minutes in Figure-3.5 [Campbell et al.(2015)] [Marcano et al (2021)].

MGAB-V1240 is an Algol type eclipsing WD binary where strong reflection is present[4]. The companion revolves around a WD candidate at 52.02 minutes [Masci et al.(2019)]. Figure-3.5 represents clear light curves with the correct period, 52.02 minutes.

ZTF18aaokmww is categorized as either CV or δ Scuti variable by ALeRCE[5]. However, the light curve indicates that the system is more likely an AM Herculis-type variable than a δ Scuti variable. Light curves in Figure-3.5 have distinct features and predicted the correct period.

ZTF18aabeviz, also known as SDSS J142430.40+440559.2, discovered by Sloan Digital Sky Survey Data Release 7 [Girven et al.(2011)], also appeared in [Jiménez-Esteban(2018)]. The companion evolves around a He-WD every 80.93 minutes [Jiménez-Esteban(2018)]. Figure-3.5 includes light curves from both algorithms with proper identification of 80.93 minutes of the orbital period.

[4]https://sites.google.com/view/mgab-astronomy/mgab-v1201-v1250#h.xmgjk03rsew5
[5]https://alerce.online/object/ZTF18aaokmww

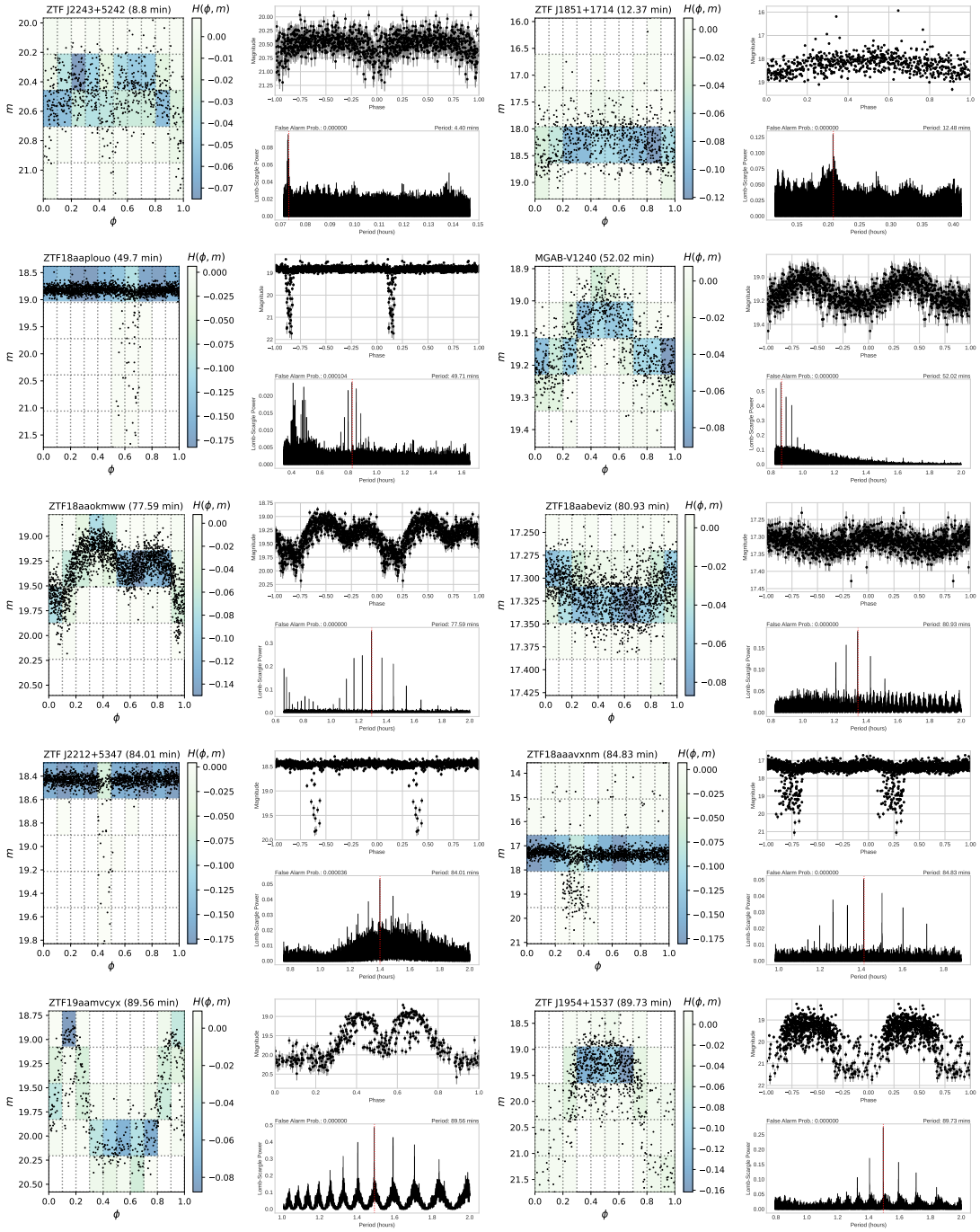

Figure 3.5: Sources from Table-3.2 used for testing Conditional Entropy and Lomb-Scargle periodograms.

ZTF J2212+5347 is an Algol type deep eclipsing binary with MS companion

Table 3.2: Binary WDs with a period under 90 minutes from the Zwicky Transient Facility (ZTF) DR3. Objects with "*" are candidates.

Source Name	RA-DEC (deg)	Type	P (min)
ZTF J2243+5242	340.92905 +52.70166	DWD	8.8
ZTF J1851+1714	282.91586 +17.24174	WDP	12.37
ZTF18aaplouo	242.89151 +63.14214	UG+E	49.7
MGAB-V1240	328.63492 +63.69845	WD*	52.02
ZTF18aaokmww	272.02155 +58.16996	AM CVn	77.59
ZTF18aabeviz	216.12656 +44.09988	WD*	80.93
ZTF J2212+5347	333.11234 +53.79743	EA/WD	84.01
ZTF18aaavxnm	225.67036 +33.57318	UGSU+E	84.83
ZTF19aamvcyx	285.20874 +40.83794	UG/DN	89.56
ZTF J1954+1537	298.72632 +15.63326	CV	89.73

E: eclipsing, **WD**: white dwarf, **DWD**: double white dwarf, **sdB**: subdwarf B-type, **AM CVn**: AM Canum Venaticorum **WDP**: White Dwarf pulsar, **UG**: U Geminorum type variable, **UGSU**: SU Ursae Majoris-type variable, **DN**: Dwarf Nova, **CV**: Cataclysmic Variable

that is identified with 84 minutes of orbital period [Keller et al.(2022)]. Light curves are plotted by both periodograms precisely have the correct period in Figure-3.5.

ZTF18aaavxnm The Sloan Digital Sky Survey observed the system in 2006 as an eclipsing SU Ursae Majoris-type variable, SDSS J150240.98+333423.9, with a period of 84.8 minutes [Szkody et al.(2006)] [Drake et al.(2009)]. A super out-

burst of at least 3.9 magnitudes that lasted 16 days was also detected in 2009 [Shears et al.(2011)]. The mass ratio of the binary system is 0.109, while the mass of WD is 0.82 M$\odot$ [Littlefair et al.(2008)]. The system has a $\sim$ 3 magnitude deep eclipse, which is correctly presented by both periodograms in Figure-3.5.

ZTF19aamvcyx(Gaia20eio) is a U Geminorum-type variable (dwarf nova), discovered by ALeRCE ZTF Explorer [Hodgkin et al.(2020)]. The orbital period of the system is obtained as 89.56 minutes [Drake et al.(2009)]. Lomb-Scargle and Conditional Entropy techniques confirmed this finding in Figure-3.5.

ZTF J1954+1537, H1907 + 609, is an eclipsing AM Herculis-type variable and an 89.7 minutes orbital period [Remillard et al.(1991)] [Masci et al.(2019)] [Chen et al.(2020)]. The system emits X-rays with long-term variability and exhibits mass transfer from MS companion [Remillard et al.(1991)]. Conditional Entropy and Lomb-Scargle periodograms agreed with that conclusion in Figure-3.5.

ZTF J1321+5609 is an AM Herculis first discovered by [Drake et al.(2009)] and also classified by [Chen et al.(2020)]. [Littlefield et all.(2015)] discussed that an accretion disk does not form around the WD, matter directly flows to magnetic poles through magnetic field lines, instead. There are no issues to obtain the correct period for both periodograms. In the case of Lomb-Scargle, many harmonics of the period can be seen in Figure-3.6.

ZTF18aahvhsb, 2XMMp J131223.4+173659, first observed in X-ray by XMM Newton [Vogel et al.(2008)]. The system is an AM Herculis-type variable that shows a deep eclipse with 91.8 minutes of period [Vogel et al.(2008)] [Drake et al.(2009)].

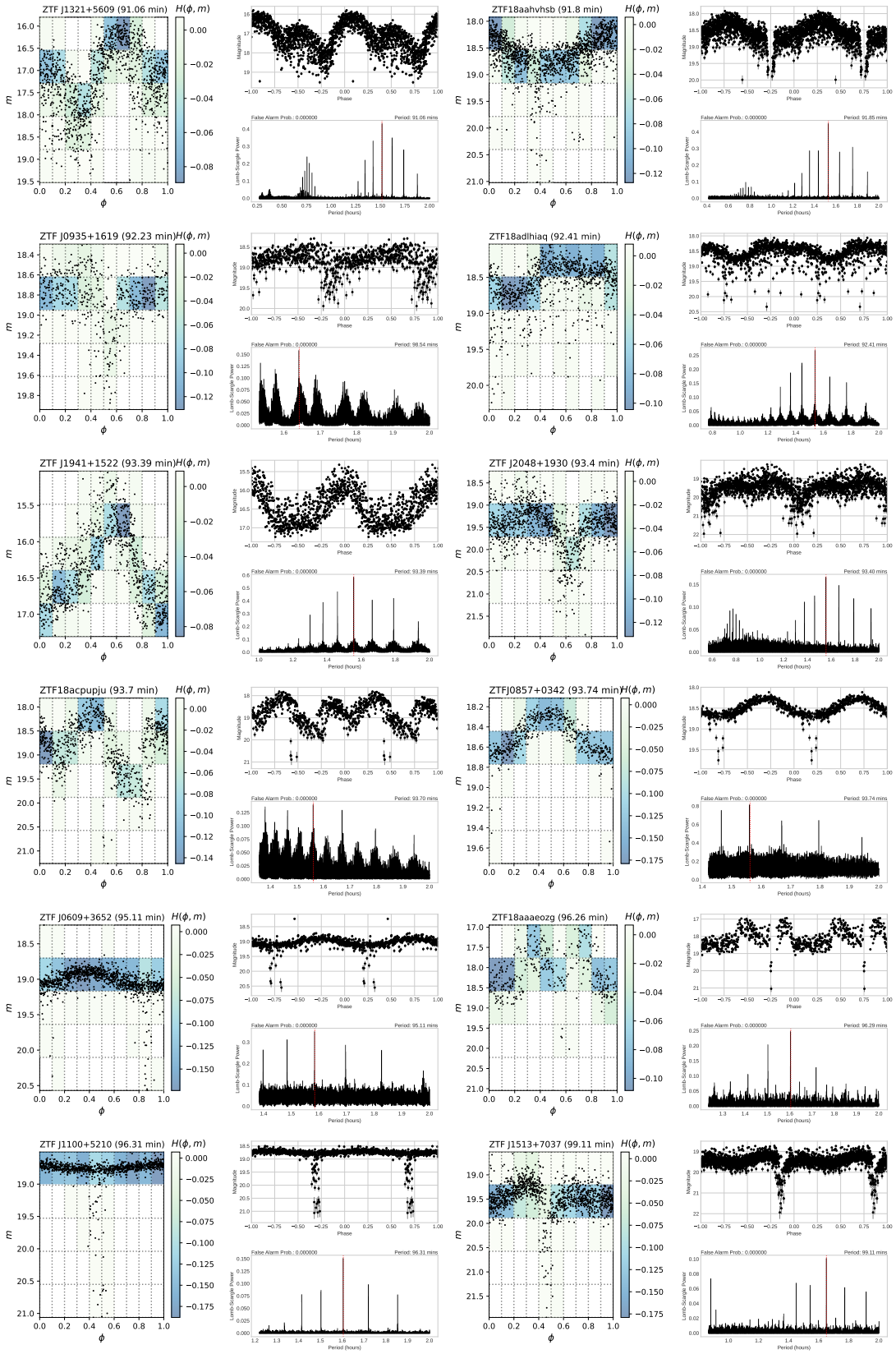

Figure 3.6: The sources from Table-3.3 used for testing Conditional Entropy and Lomb-Scargle periodograms.

[Vogel et al.(2008)] also discusses accretion and X-ray emission lack of soft components. Light curves in Figure-3.6 are clean and have correct periods.

ZTF J0935+1619 classified as an eclipsing CV, novalike with large accretion rate, and a magnetic WD as primary star [Szkody et al.(2009)]. However, the orbital period (92.23 minutes) of the system is first mentioned in [Southworth et al.(2015)]. ZTF identification is done by [Keller et al.(2022)]. Light curves from different algorithms in Figure-3.6 are in agreement that the orbital period is 92.23 minutes.

ZTF18adlhiaq is classified as AM Herculis with an orbital period of 92.41 minutes[Masci et al.(2019)]. Plots from Lomb-Scargle and Conditional Entropy periodograms are shown in Figure-3.6.

ZTF J1941+1522 is assigned as an AM Herculis in ZTF survey [Masci et al.(2019)]. It is also known as ASASSN-V J194125.07+152255.4, first observed as a non-periodic variable[6]. However, it is speculated that the system could be a Dwarf Nova[7]. Light curves indicate that the source has a period of 93.39 minutes in Figure-3.6.

ZTF J2048+1930 appeared in ZTF observations as AM Herculis type variable at a period of 93.4 minutes [Masci et al.(2019)] [Keller et al.(2022)]. The system shows rotational variability and a broad cyclotron hump in the spectrum confirms the classification [Keller et al.(2022)]. Lomb-Scargle and Conditional Entropy periodograms demonstrate light curves that indicate the period is indeed 93.4 minutes, see Figure-3.6.

[6]https://asas-sn.osu.edu/variables94c0807a-beeb-5105-a81b-fc08c34376ad
[7]http://ooruri.kusastro.kyoto-u.ac.jp/mailarchive/vsnet-chat/8009

Table 3.3: Binary samples with a period between 90-100 minutes from the Zwicky Transient Facility (ZTF) DR3.

Source Name	RA-DEC (deg)	Type	P (min)
ZTF J1321+5609	200.26677 +56.16610	AM	91.06
ZTF18aahvhsb	198.09787 +17.61648	AM+E	91.8
ZTF J0935+1619	143.90608 +16.33079	CV+E	92.23
ZTF18adlhiaq	318.21439 +32.63265	AM	92.41
ZTF J1941+1522	295.35413 +15.38182	AM	93.39
ZTF J2048+1930	312.18625 +19.50543	CV	93.4
ZTF18acpupju	121.03306 -0.37118	CV	93.7
ZTF J0857+0342	134.44243 +3.71542	EA/WD	93.74
ZTF J0609+3652	92.30993 +36.86746	EA/WD	95.11
ZTF18aaaeozg	32.37423 +28.54134	AM+E	96.26
ZTF J1100+5210	165.18806 +52.17881	EA/WD	96.31
ZTF J1513+7037	228.38737 +70.62289	UG+E	99.1

E: eclipsing, **AM CVn**: AM Canum Venaticorum **EA**: Eclipsing Algol type variable, **UG**: U Geminorum type variable, **UGSU**: SU Ursae Majoris-type variable, **DN**: Dwarf Nova, **CV**: Cataclysmic Variable.

ZTF18acpupju is a CV that has a period of 93.7 minutes [Masci et al.(2019)]. Figure-3.6 shows light curves generated by Lomb-Scargle and Conditional Entropy periodograms.

ZTF J0857+0342 is an Algol type eclipsing binary, first appeared in Catalina Sur-

vey [Drake et al.(2009)]. The period of the system is 93.74 minutes [Drake et al.(2009)]. ZTF J0857+0342 has a light curve with a clear eclipse in Figure-3.6.

ZTF J0609+3652 is an Algol type binary with 95.1 minutes period [Masci et al.(2019)]. Light curves in Figure-3.6 display a clear eclipse pattern.

ZTF18aaaeozg is an eclipsing X-ray source first discovered in [Denisenko et al.(2006)], and appeared in [Drake et al.(2009)] as an AM Herculis type variable. The primary is a WD with a strong magnetic field and the companion is a red M6 V star [Denisenko et al.(2006)]. Light curves shown in Figure-3.6 exhibit a clear pattern of the eclipse with the correct period.

ZTF J1100+5210 is an eclipsing WD binary, SDSS J110045.15+521043.8, first reported in [Kepler et al.(2015)]. The orbital period is 96.31 minutes in Figure-3.6 and there is a ~ 3 magnitude deep eclipse in the system [Masci et al.(2019)].

ZTF J1513+7037 is another CV, identified as an eclipsing U Geminorum (Dwarf Nova) type variable, represented by [Masci et al.(2019)] and [Keller et al.(2022)]. The period is determined by the Lomb-Scargle periodogram as 99.11 minutes [Keller et al.(2022)], which is also verified in Fig-3.6 by the conditional entropy method.

ZTF18aboonvu is an eclipsing binary that includes a WD as the primary star [Jiménez-Esteban(2018)]. Light curves show the correct period in Figure-3.7.

ZTF18aaxcnxg is an eclipsing AM Herculis variable [Remillard et al.(1991)]. Conditional Entropy and Lomb-Scargle methods confirm that the period is 104.62 minutes (see Figure-3.7).

ZTF J1844+4857 and **ZTF18aapjwvr** are Algol type eclipsing WD binaries

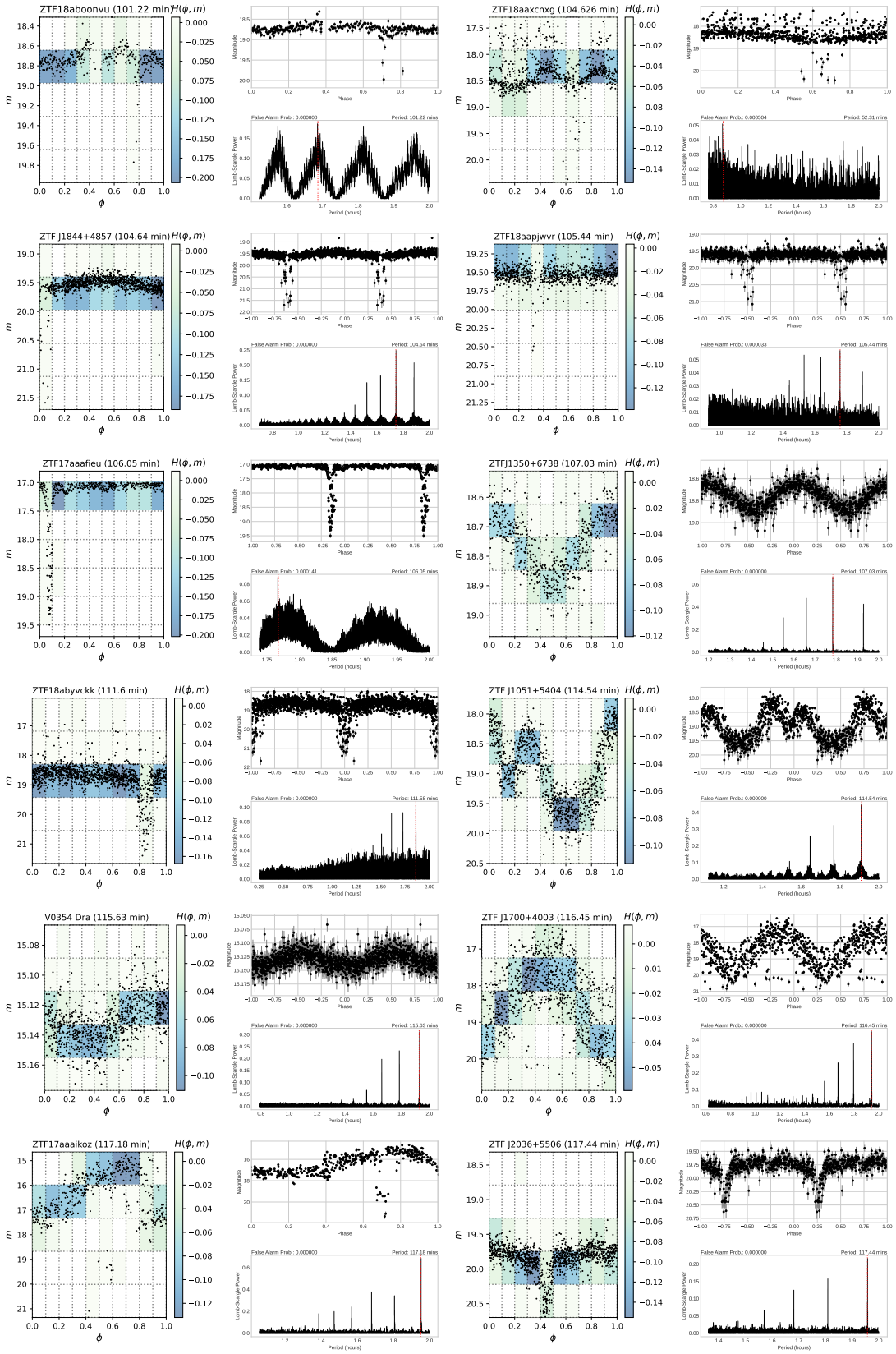

Figure 3.7: Sources from Table-3.4 used for testing Conditional Entropy and Lomb-Scargle periodograms.

in ZTF Survey [Masci et al.(2019)]. In Figure-3.7, these systems have periods of 104.64 and 105.44 minutes, respectively.

ZTF17aaafieu is an eclipsing X-ray source, U Geminorum-type variable, that produces Dwarf Nova Oscillations (DNOs) [Patterson et al.(1981)]. Light curves display that the source dims 2.5 magnitudes during the eclipse, and an orbital period of 106.05 minutes is seen in Figure-3.7.

ZTFJ1350+6738 is a W UMa type variable that has a period of 107.03 minutes [Chen et al.(2020)], in Figure-3.7.

ZTF18abyvckk is another SU Ursae Majoris-type variable with 111.6 minutes period [Forster et al.(2021)]. Light curves show that the system has ~ 4 magnitude deep eclipse in Figure-3.7.

ZTF J1051+5404 has a period 114.54 minutes [Morris et al.(1987)] [Drake et al.(2009)] [Chen et al.(2020)]. The system contains a rotating magnetized WD with strong circular polarization and continuous X-ray and optical emission [Morris et al.(1987)]. The distinctive pattern in light curves, Figure-3.7, represents that the system is an AM Herculis-type binary.

V0354 Dra includes a magnetic WD that has a dark spot on the surface and shows rotational variability [Brinkworth et al.(2004)]. Both periodograms agree on an orbital period is 115.63 minutes in Figure-3.7.

ZTF J1700+4003 is first observed in an X-ray band rather than an optical band and identified as AM Herculis type eclipsing binary [Homer et al.(2005)]. A big amplitude change, ~ 4 magnitudes, is observed in the light curve in Figure-3.7.

V0808 Aur is an AM Herculis type WD+DM pair that is observed by Catalina

Table 3.4: Binary WDs from with a period bigger than 100 minutes the Zwicky Transient Facility (ZTF) DR3. Sources with * are candidates.

Source Name	RA-DEC (deg)	Type	P (min)
ZTF18aboonvu	286.03912 -27.68042	WD*	101.2
ZTF18aaxcnxg	286.77606 +69.14574	AM+E	104.626
ZTF J1844+4857	281.14334 +48.96016	EA/WD	104.64
ZTF18aapjwvr	217.47249 +52.39835	EA/WD	105.44
ZTF17aaafieu	17.55491 +60.07649	UGSU+E	106.05
ZTF J1350+6738	207.73439 +67.64373	EW	107.03
ZTF18abyvckk	309.39423 +26.28250	UGSU	111.6
ZTF J1051+5404	162.89633 +54.07664	AM/CV	114.54
V0354 Dra	250.23711 +53.68499	ROT/WD	115.63
ZTF J1700+4003	255.22212 +40.06601	AM/CV	116.45
ZTF17aaaikoz	107.85819 +44.06806	AM+E	117.18
ZTF J2036+5506	309.00693 +55.11357	EA/WD	117.44

E: eclipsing, **WD**: white dwarf, **AM CVn**: AM Canum Venaticorum, **UGSU**: SU Ursae Majoris-type variable, **CV**: Cataclysmic Variable **ROT**: Rotating, **EW**: W Uma type variable

Real-Time Transient Survey [Drake et al.(2009)] [Thorne et al.(2010)]. The system has a period of 117.44 minutes [Drake et al.(2009)] [Thorne et al.(2010)]. Figure-3.7 shows a bright light curve with a visible dip.

ZTF J2036+5506 is a binary system formed as a White Dwarf with an MS companion, and its orbital period is 117.44 minutes [Keller et al.(2022)]. However,

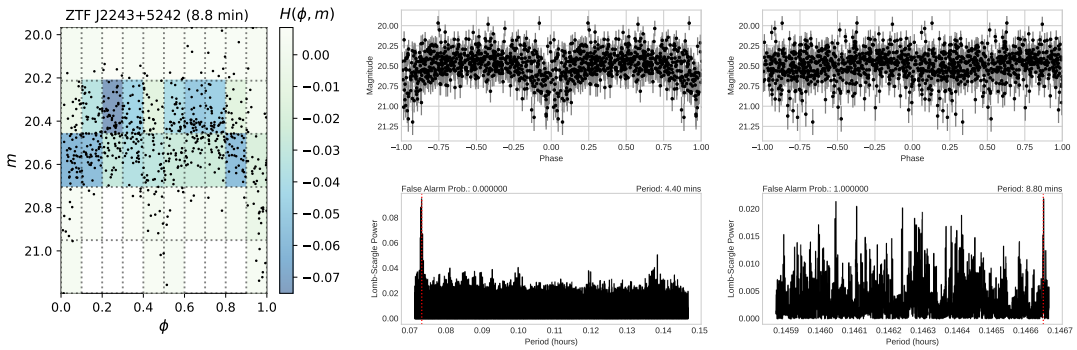

Figure 3.8: Lomb-Scargle and Conditional Entropy periodograms for ZTF J2243+5242. The light curve with half of the correct period is in middle, and the light curve with the correct period is on right.

[Chen et al.(2020)] indicated that it is an Algol-type eclipsing system with a period of 3.91 hours in the ZTF collection of periodic variable stars. Lomb-Scargle and Conditional Entropy successfully extracted the proper period from the data in Figure-3.7.

In section-3.3, I compared Conditional Entropy (CE) and Lomb-Scargle (LS) periodogram for 34 WD binaries, in Figure-3.5-3.7. The Conditional Entropy periodogram successfully plotted the light curves and found the correct periods for all sources. Lomb-Scargle periodogram predicted all the orbital periods and light curves except for ZTF J2243+5242, in Figure-3.8. The figure shows that the Lomb-Scargle periodogram could not plot a clean light curve at a period of 8.8 minutes. The Lomb-Scargle periodogram misidentified the correct period as its half value.

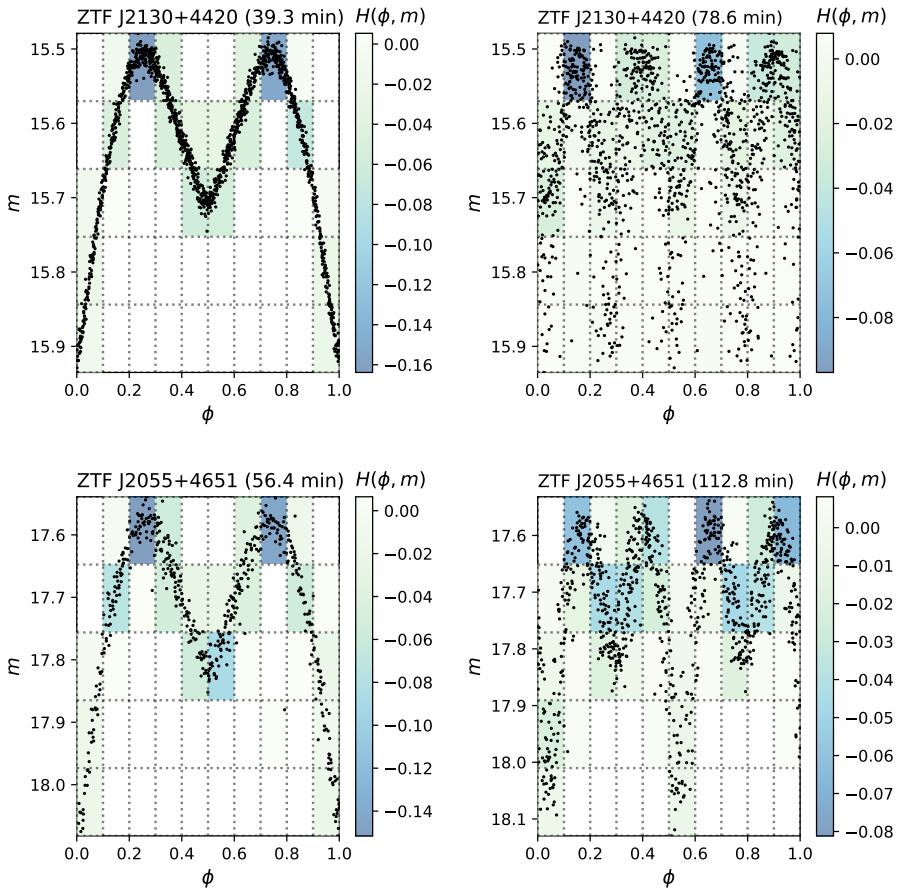

Figure 3.9: Conditional Entropy periodogram plots the correct period and its harmonic for ZTF J2130+4420 and ZTF J2055+4651.

We stated that the Lomb-Scargle periodogram has an issue identifying the correct period and its harmonics. One may ask the same question for the Conditional Entropy algorithm. Figure-3.9 provides two examples of harmonic detection in Conditional Entropy. In this case, the periodogram can identify objects with two different periods. However, the Conditional Entropy measurement, $H(\phi, m)$, is a distinctive feature that can separate the correct period from its harmonics.

3.4 Results

I searched for white dwarf binaries with periods less than two hours in ZTF DR3. I aim to conduct a preliminary evaluation of the Conditional Entropy approach and compare two unique period-finding methods.

The analysis began with testing proficiency of the Conditional Entropy periodogram. 15 sources from [Burdge et al.(2020b)] are identified accurately by the Conditional Entropy periodogram in Figure-3.1. Lomb-Scargle periodogram, on the other hand, identified only 7 of them correctly, Figure-3.2. The remaining sources, in Figure-3.3 and 3.4, were determined as the harmonics of the periods are the actual periods.

Figure-3.2 represents the sources where both Conditional Entropy and Lomb-Scargle periodograms accurately estimated the correct periods. However, [Burdge et al.(2020b)] used the Lomb-Scargle periodogram only in bootstrapping testing to determine the uncertainties in the orbital period.

In Figure-3.3 and 3.4, there are no distinctive characteristics among the sources that would be a problem for the Lomb-Scargle period finding algorithm. The remaining sources are interacting binary WDs, either eclipsing or ellipsoidal variables. Lomb-Scargle periodogram fitted all light curves with correct periods, except PTF J0533+0209, ZTF J1749+0924, and ZTF J2320+3750 in Figure-3.4. However, Lomb-Scargle power and false alarm probability indicated that the periods are incorrect. ZTF J0640+1738 and ZTF J1901+5309 differ from others by having the correct light curves with the actual period, yet, the false alarm

probabilities are above the accepted limit ($\leq 10\%$). The reason is that there is no analytical solution for false alarm probability [Vanderplas(2018)]. Methods like bootstrapping and false alarm probability ([Baluev(2007)]) are simple numerical solutions that do not work for every single object. On the other hand, the harmonics of the periods appear to be correct period.

The Conditional Entropy periodogram agreed with the literature on all periods and light curves for WD binaries ($P \leq 2$ hours) selected from ZTF DR3. Lomb-Scargle periodogram, on the other hand, performed poorly on six sources. ZTF J0640+1738 and ZTF J1901+5309 are excluded because they found periods that fall below the detection limit with a high false alarm probability. ZTF J2243+5242 is the only disagreement between algorithms on ZTF DR3 samples. The correct period was identified by the Lomb-Scargle periodogram in Figure-3.8, although the algorithm was ineffective in producing an accurate light curve.

3.5 Discussion and Conclusion

This thesis relies on how well the Conditional Entropy algorithm works and comparison to the Lomb-Scargle periodogram. I used ZTF Data Release 3 to compare the outcomes of two period-finding approaches. To calculate the orbital period of eclipsing binaries, we utilized the Conditional Entropy code, a `Python` module under `cuvarbase`, which was initially created by John Hoffman in 2017 (`https://github.com/johnh2o2/cuvarbase`). One concern with other period-finding algorithms, particularly for the Lomb–Scargle periodogram, is the misiden-

tification of harmonics as the accurate period, as noted in [Graham et al.(2013a)]. The actual period and half-period are not statistically distinct for symmetric eclipsing binary systems [Graham et al.(2013a)]. It is likely that the Lomb-Scargle periodogram, on detection of harmonics, detects half the orbital period. The Conditional Entropy algorithm, on the contrary, obtains twice the orbital period. Conditional Entropy, unlike the Lomb-Scargle periodogram, except ZTF J0640+1738 and ZTF J1901+5309, can detect harmonics along with the actual period and distinguish the genuine period from its harmonics by measuring entropy levels. Identifying the orbital period of binary systems with secondary eclipse is the most prevalent challenge in our data set [Graham et al.(2013a)]. The Lomb-Scargle periodogram has correct identifications for 7 short-period WD binaries out of 15 systems [Burdge et al.(2020b)]. Misidentified sources include 5 eclipsing binary and 3 ellipsoidal variables. There is also one object, ZTF J2243+5242, that peak frequency in the periodogram determination is incorrect. The Conditional Entropy method, conversely, found the correct period. Furthermore, the Conditional Entropy approach relies less on noise in data collection, and it finds periodicity for harmonic data at all noise levels. It is shown in Figure-3.9 that the Conditional Entropy periodogram can distinguish the correct period from its harmonics.

From the computational perspective, Lomb-Scargle ($\mathcal{O}(n^2)$) is more expensive than Conditional Entropy ($\mathcal{O}(nN)$), where n is the number of observations and N is the number of tested frequencies [Vanderplas(2018)] [Graham et al.(2013b)]. There is also no exact binning strategy, bin width, or the number of bins to

generate light curves. All the period-finding methods initially depend on data quality, the number of good observations, and the signal-to-noise ratio. Moreover, if one is only interested in detecting periodic behavior, then $\sim 70\%$ of objects in a survey would be identified with correct periods [Graham et al.(2013b)].

References

[Baluev(2007)] Baluev, R. V., "Assessing the statistical significance of periodogram peaks", Monthly Notices of the Royal Astronomical Society, vol. 385, no. 3, pp. 1279–1285, 2008. doi:10.1111/j.1365-2966.2008.12689.x.

[Bellm(2014)] Bellm, E., "The Zwicky Transient Facility", in The Third Hot-wiring the Transient Universe Workshop, 2014, pp. 27–33.

[Bellm et al.(2018)] Bellm, E. C., Kulkarni, S. R., Graham, M. J., Dekany, R., Smith, R. M., Riddle, R., ... Adams, S. M.(2018). The Zwicky Transient Facility: System Overview, Performance, and First Results. Publications of the Astronomical Society of the Pacific, 131(995), 018002. doi:10.1088/1538-3873/aaecbe

[Bellotti et al.(2020)] Bellotti, S., Zabludoff, A. I., Belikov, R., Guyon, O., and Rathi, C., "Detecting Exoplanets Using Eclipsing Binaries as Natural Starshades", The Astronomical Journal, vol. 160, no. 3, 2020. doi:10.3847/1538-3881/aba7c6.

[Benz et al.(1990)] Benz, W., Bowers, R. L., Cameron, A. G. W., and Press, W. H., "Dynamic Mass Exchange in Doubly Degenerate Binaries. I. 0.9 and 1.2 $M_{\odot}$ Stars", The Astrophysical Journal, vol. 348, p. 647, 1990. doi:10.1086/168273.

[Bienias et al.(2021)] Bienias, J., Bódi, A., Forró, A., Hajdu, T., and Szabó, R., "Background Short-period Eclipsing Binaries in the Original Kepler Field", The Astrophysical Journal Supplement Series, vol. 256, no. 1, 2021. doi:10.3847/1538-4365/ac10c0.

[Boss(1910)] Boss, L.(1910). Preliminary General Catalogue of 6188 stars for the epoch 1900. Carnegie Institution of Washington.

[Box and Jenkins(1970)] Box, G.E.P. and Jenkins, G.M.(1970) Time Series Analysis: Forecasting and Control. Holden-Day, San Francisco

[Brown et al.(2010)] Brown, W. R., Kilic, M., Allende Prieto, C., and Kenyon, S. J., "The ELM Survey. I. A Complete Sample of Extremely Low-mass White Dwarfs", The Astrophysical Journal, vol. 723, no. 2, pp. 1072–1081, 2010. doi:10.1088/0004-637X/723/2/1072.

[Brinkworth et al.(2004)] Brinkworth, C. S., Burleigh, M. R., Wynn, G. A., and Marsh, T. R., "Photometric variability of the unique magnetic white dwarf GD 356", Monthly Notices of the Royal Astronomical Society, vol. 348, no. 3, pp. L33–L37, 2004. doi:10.1111/j.1365-2966.2004.07538.x.

[Burdge et al.(2019a)] Burdge, K., "ZTF J1539+5027: the Shortest Period Eclipsing White Dwarf Binary", HST Proposal, p. 15897, 2019.

[Burdge et al.(2019b)] Burdge, K. B., "Orbital Decay in a 20 Minute Orbital Period Detached Binary with a Hydrogen-poor Low-mass White Dwarf", The Astrophysical Journal, vol. 886, no. 1, 2019. doi:10.3847/2041-8213/ab53e5.

[Burdge et al.(2020a)] Burdge, K. B., "An 8.8 Minute Orbital Period Eclipsing Detached Double White Dwarf Binary", The Astrophysical Journal, vol. 905, no. 1, 2020. doi:10.3847/2041-8213/abca91.

[Burdge et al.(2020b)] Burdge, K. B., "A Systematic Search of Zwicky Transient Facility Data for Ultracompact Binary LISA-detectable Gravitational-wave Sources", The Astrophysical Journal, vol. 905, no. 1, 2020. doi:10.3847/1538-4357/abc261

[Campbell et al.(2015)] Campbell, H. C., "Total eclipse of the heart: the AM CVn Gaia14aae/ASSASN-14cn", Monthly Notices of the Royal Astronomical Society, vol. 452, no. 1, pp. 1060–1067, 2015. doi:10.1093/mnras/stv1224

[Catelan and Smith(2015)] Catelan, M. and Smith, H. A., "Pulsating Stars", Wiley, 2015, ISBN: 9783527655182.

[Chandrasekhar(1931)] Chandrasekhar, S., "The Maximum Mass of Ideal White Dwarfs", The Astrophysical Journal, vol. 74, p. 81, 1931. doi:10.1086/143324.

[Chen et al.(2020)] Chen, X., Wang, S., Deng, L., de Grijs, R., Yang, M., and Tian, H., "The Zwicky Transient Facility Catalog of Periodic Variable Stars", The Astrophysical Journal Supplement Series, vol. 249, no. 1, 2020. doi:10.3847/1538-4365/ab9cae.

[Cincotta et al.(1995)] Cincotta, Pablo M., et al. "Astronomical Time Series Analysis. I. A Search for Periodicity Using Information Entropy." The Astrophysical Journal, vol. 449, Aug. 1995, p. 231., https://doi.org/10.1086/176050.

[Cincotta et al.(1999a)] Cincotta, Pablo M., et al. "Astronomical time-series analysis – II. A search for periodicity using the Shannon entropy" Monthly Notices of the Royal Astronomical Society, vol. 302, no. 3, Aug. 1999, pp. 302, 582. doi:10.1046/j.1365-8711.1999.02128.x

[Cincotta et al.(1999b)] Cincotta, Pablo M., et al. "Astronomical Time-Series Analysis — III. The Role of the Observational Errors in the Minimum Entropy Method." Monthly Notices of the Royal Astronomical Society, vol. 307, no. 4, Aug. 1999, pp. 941–48., https://doi.org/10.1046/j.1365-8711.1999.02667.x.

[Coughlin et al.(2020)] Coughlin, M. W., "ZTF J1901+5309: a 40.6-min orbital period eclipsing double white dwarf system", Monthly Notices of the Royal Astronomical Society, vol. 494, no. 1, pp. L91–L96, 2020. doi:10.1093/mnrasl/slaa044.

[Cox(1980)] Cox, John P. Theory of Stellar Pulsation. Princeton University Press, 1980.

[De Marchi et al.(2004)] De Marchi, G., Paresce, F., Straniero, O., and Prada Moroni, P. G., "On the age and mass function of the globular cluster M 4: A different interpretation of recent deep HST observations", Astronomy and Astrophysics, vol. 415, pp. 971–985, 2004. doi:10.1051/0004-6361:20031588.

[Denisenko et al.(2006)] Denisenko, D. V., Pavlinsky, M. N., Sunyaev, R. A., Aslan, Z., Khamitov, I., and Parmaksizoglu, M., "Deep eclipses in the cataclysmic variable 1RXS J020929.0+283243", Astronomy Letters, vol. 32, no. 4, pp. 252–256, 2006. doi:10.1134/S1063773706040050.

[Drake et al.(2009)] Drake, A. J., et al. "First Results from the Catalina Real-Time Transient Survey", The Astrophysical Journal, vol. 696, no. 1, pp. 870–884, 2009.

[Drake et al. 2014] Drake, A. J., et al. "The Catalina Surveys Periodic Variable Star Catalog", The Astrophysical Journal Supplement Series, vol. 213, no. 1, 2014. doi:10.1088/0067-0049/213/1/9.

[Eddington(1922)] Eddington, A. S., "Society Business: Introductory address delivered on the occasion of the Society's centenary celebration", Monthly Notices of the Royal Astronomical Society, vol. 82, p. 432, 1922. doi:10.1093/mnras/82.7.432.

[Eddington(1940)] Eddington, A. S., "The physics of white dwarf matter", Monthly Notices of the Royal Astronomical Society, vol. 100, p. 582, 1940. doi:10.1093/mnras/100.8.582.

[Ellerman(2022)] Ellerman, D. New Foundations of Information Theory: Logical Entropy and Shannon Entropy. 2022, Springer Pub., https://doi.org/10.1007/978-3-030-86552-8.

[Feigelson et al.(2018)] Feigelson, E. D., Babu, G. J., and Caceres, G. A., "Autoregressive Times Series Methods for Time Domain Astronomy", Frontiers in Physics, vol. 6, 2018. doi:10.3389/fphy.2018.00080.

[Fowler(1926)] Fowler, R. H., "On dense matter", Monthly Notices of the Royal Astronomical Society, vol. 87, pp. 114–122, 1926. doi:10.1093/mnras/87.2.114.

[Fourier(1822)] Fourier J. B. J., "The analytical Theory of Heat", Cambridge University Press, 2009 (Re-issued), ISBN: 9781108001786

[Forster et al.(2021)] Förster, F., "The Automatic Learning for the Rapid Classification of Events (ALeRCE) Alert Broker", The Astronomical Journal, vol. 161, no. 5, 2021. doi:10.3847/1538-3881/abe9bc.

[Frank, King & Raine(2002)] Frank, J., King, A., Raine, D., Accretion Power in Astrophysics (Third ed.), (2002). Cambridge University Press. ISBN 0-521-62957-8.

[Fu et al. (2021)] Fu, Jinbo, Xinhao He, and Tuan Yi. "Deep Learning Techniques for Eclipsing Binary Light Curves Classification." (2021).

[Girven et al.(2011)] J. Girven, B. T. Gänsicke, D. Steeghs, D. Koester, DA white dwarfs in Sloan Digital Sky Survey Data Release 7 and a search for infrared excess emission, Monthly Notices of the Royal Astronomical Society, Volume 417, Issue 2, October 2011, Pages 1210–1235, https://doi.org/10.1111/j.1365-2966.2011.19337.x

[Graham et al.(2013a)] Graham, Matthew J., et al. "A Comparison of Period Finding Algorithms." Monthly Notices of the Royal Astronomical Society, vol. 434, no. 4, Oct. 2013, pp. 3423–44., https://doi.org/10.1093/mnras/stt1264.

[Graham et al.(2013b)] Graham, Matthew J., et al. "Using Conditional Entropy to Identify Periodicity." Monthly Notices of the Royal Astronomical Society, vol. 434, no. 3, Sept. 2013, pp. 2629–35., https://doi.org/10.1093/mnras/stt1206.

[Graham et al.(2019)] Matthew J. Graham et al., "The Zwicky Transient Facility: Science Objectives", Publications of Astronomical Society of the Pacific, 131:078001 (23pp), 2019 July, doi:10.1088/1538-3873/ab006c.

[Gong et al.(2018)] Gong, Y.-X. and Ji, J., "Formation of S-type planets in close binaries: scattering-induced tidal capture of circumbinary planets", Monthly Notices of the Royal Astronomical Society, vol. 478, no. 4, pp. 4565–4574, 2018. doi:10.1093/mnras/sty1300.

[Goodricke(1783)] Goodricke John 1783XXVI. A series of observations on, and a discovery of, the period of the variation of the light of the bright star in the head of medusa, called algol. In a letter from John Goodricke, Esq. to the Rev. Anthony Shepherd, D. D. F. R. S. and Plumian Professor at CambridgePhil. Trans. R. Soc.73474–482.

[Hansen et al.(2002)] Hansen, B. M. S., "The White Dwarf Cooling Sequence of the Globular Cluster Messier 4", The Astrophysical Journal, vol. 574, no. 2, pp. L155–L158, 2002. doi:10.1086/342528.

[Hartmann(2008)] Hartmann, L. (2008). Accretion Processes in Star Formation (2nd ed., Cambridge Astrophysics). Cambridge: Cambridge University Press. doi:10.1017/CBO9780511552090

[Hernandez(1999)] Hernandez, G. "Time Series, Periodograms, and Significance." Journal of Geophysical Research: Space Physics, vol. 104, no. A5, May 1999, pp. 10355–68., https://doi.org/10.1029/1999JA900026.

[Herschel(1785)] Herschel, W.(1785). "Catalogue of Double Stars". Philosophical Transactions of the Royal Society of London. 75: 40–126. doi:10.1098/rstl.1785.0006.

[Hillebrandt et al.(2000)] Hillebrandt, W. and Niemeyer, J. C., "Type IA Supernova Explosion Models", Annual Review of Astronomy and Astrophysics, vol. 38, pp. 191–230, 2000. doi:10.1146/annurev.astro.38.1.191.

[Hodgkin et al.(2020)] Hodgkin, S. T., "GaiaAlerts Transient Discovery Report for 2020-09-17", TNSTR2833, 2020.

[Homer et al.(2005)] Homer, L., "XMM-Newton and Optical Follow-up Observations of Three New Polars from the Sloan Digital Sky Survey", The Astrophysical Journal, vol. 620, no. 2, pp. 929–937, 2005. doi:10.1086/427260.

[Jiménez-Esteban(2018)] Jiménez-Esteban, F. M., "A white dwarf catalogue from Gaia-DR2 and the Virtual Observatory", Monthly Notices of the Royal Astronomical Society, vol. 480, no. 4, pp. 4505–4518, 2018. doi:10.1093/mnras/sty2120.

[José(2016)] Jose, Jordi. Stellar Explosions: Hydrodynamics and Nucleosynthesis. CRC Press Taylor Francis Group, 2016.

[Kalman(1960)] Kalman, R. E. (1960). A New Approach to Linear Filtering and Prediction Problems. Journal of Basic Engineering, 82(1), 35. doi:10.1115/1.3662552

[Kallrath & Milone(2009)] Kallrath, Josef, and E. F. Milone. Eclipsing Binary Stars: Modeling and Analysis. Springer, 2009. doi:10.1007/978-1-4757-3128-6

[Kato & Kojiguchi(2021)] Kato, T. and Kojiguchi, N., "ZTF J185139.81+171430.3 = ZTF18abnbzvx: the second white dwarf pulsar?", arXiv e-prints, 2021. doi:10.48550/arXiv.2107.09913.

[Keller et al.(2022)] Keller, P. M., "Eclipsing white dwarf binaries in Gaia and the Zwicky Transient Facility", Monthly Notices of the Royal Astronomical Society, vol. 509, no. 3, pp. 4171–4188, 2022. doi:10.1093/mnras/stab3293.

[Kepler et al.(2007)] Kepler, S. O., "White dwarf mass distribution in the SDSS", Monthly Notices of the Royal Astronomical Society, vol. 375, no. 4, pp. 1315–1324, 2007. doi:10.1111/j.1365-2966.2006.11388.x.

[Kepler et al.(2015)] Kepler, S. O., "New white dwarf stars in the Sloan Digital Sky Survey Data Release 10", Monthly Notices of the Royal Astronomical Society, vol. 446, no. 4, pp. 4078–4087, 2015. doi:10.1093/mnras/stu2388.

[Kilic et al.(2007)] Kilic, M., Allende Prieto, C., Brown, W. R., and Koester, D., "The Lowest Mass White Dwarf", The Astrophysical Journal, vol. 660, no. 2, pp. 1451–1461, 2007. doi:10.1086/514327.

[Kilic et al.(2010)] Kilic, M., Brown, W. R., Allende Prieto, C., Kenyon, S. J., and Panei, J. A., "The Discovery of Binary White Dwarfs that will Merge Within 500 Myr", The Astrophysical Journal, vol. 716, no. 1, pp. 122–130, 2010. doi:10.1088/0004-637X/716/1/122.

[Kilic et al.(2012)] Kilic, M., Thorstensen, J. R., Kowalski, P. M., and Andrews, J., "11-12 Gyr old white dwarfs 30 pc away", Monthly Notices of the Royal Astronomical Society, vol. 423, no. 1, pp. L132–L136, 2012. doi:10.1111/j.1745-3933.2012.01271.x.

[Kilic et al.(2017)] Kilic, M., "The Ages of the Thin Disk, Thick Disk, and the Halo from Nearby White Dwarfs", The Astrophysical Journal, vol. 837, no. 2, 2017. doi:10.3847/1538-4357/aa62a5.

[Kosakowski et al.(2022)] Kosakowski, A., Kilic, M., Brown, W. R., Bergeron, P., and Kupfer, T., "Four new deeply-eclipsing white dwarfs in ZTF", Monthly Notices of the Royal Astronomical Society, 2022. doi:10.1093/mnras/stac1146.

[Kulp(2013)] Kulp, C. W. "Detecting Chaos in Irregularly Sampled Time Series." Chaos: An Interdisciplinary Journal of Nonlinear Science, vol. 23, no. 3, Sept. 2013, p. 033110., https://doi.org/10.1063/1.4813865.

[Kupfer et al.(2020)] Kupfer, T., "The First Ultracompact Roche Lobe-Filling Hot Subdwarf Binary", The Astrophysical Journal, vol. 891, no. 1, 2020. doi:10.3847/1538-4357/ab72ff.

[Larsson(1996)] Larsson, S., "Parameter estimation in epoch folding analysis.", Astronomy and Astrophysics Supplement Series, vol. 117, pp. 197–201, 1996.

[Lieb et al.(1987)] Lieb, Elliott H., and Horng-Tzer Yau. 1987. "A Rigorous Examination of the Chandrasekhar Theory of Stellar Collapse." The Astrophysical Journal 323 (December): 140. doi:10.1086/165813.

[Littlefair et al.(2008)] Littlefair, S. P., "On the evolutionary status of short-period cataclysmic variables", Monthly Notices of the Royal Astronomical Society, vol. 388, no. 4, pp. 1582–1594, 2008. doi:10.1111/j.1365-2966.2008.13539.x.

[Littlefield et all.(2015)] Littlefield, C., "High-Amplitude, Rapid Photometric Variation of the New Polar MASTER OT J132104.04+560957.8", Information Bulletin on Variable Stars, vol. 6129, p. 1, 2015. doi:10.48550/arXiv.1412.8328.

[Liu et al.(2018)] Liu, D., Wang, B., Chen, W., Zuo, Z., and Han, Z., "Evolving ONe WD+He star systems to intermediate-mass binary pulsars", Monthly Notices of the Royal Astronomical Society, vol. 477, no. 1, pp. 384–391, 2018. doi:10.1093/mnras/sty561.

[Lomb(1976)] Lomb, N. R. "Least-Squares Frequency Analysis of Unequally Spaced Data." Astrophysics and Space Science, vol. 39, no. 2, Feb. 1976, pp. 447–62., https://doi.org/10.1007/BF00648343.

[Marcano et al (2021)] Pichardo Marcano, M., Rivera Sandoval, L. E., Maccarone, T. J., and Scaringi, S., "TACOS: TESS AM CVn Outbursts Survey", Monthly Notices of the Royal Astronomical Society, vol. 508, no. 3, pp. 3275–3289, 2021. doi:10.1093/mnras/stab2685

[Marsh et al.(1995)] Marsh, T. R., Dhillon, V. S., and Duck, S. R., "Low-Mass White Dwarfs Need Friends - Five New Double-Degenerate Close Binary Stars", Monthly Notices of the Royal Astronomical Society, vol. 275, p. 828, 1995. doi:10.1093/mnras/275.3.828.

[Masci et al.(2019)] Masci, F. J., "The Zwicky Transient Facility: Data Processing, Products, and Archive", Publications of the Astronomical Society of the Pacific, vol. 131, no. 995, p. 018003, 2019. doi:10.1088/1538-3873/aae8ac

[Miller et al.(2013)] Miller Bertolami, M. M., Althaus, L. G., and García-Berro, E., "Quiescent Nuclear Burning in Low-metallicity White Dwarfs", The Astrophysical Journal, vol. 775, no. 1, 2013. doi:10.1088/2041-8205/775/1/L22.

[Morris et al.(1987)] Morris, S. L., Schmidt, G. D., Liebert, J., Stocke, J., Gioia, I. M., and Maccacaro, T., "1E 1048.5+5421: A New 114 Minute AM Herculis Binary", The Astrophysical Journal, vol. 314, p. 641, 1987. doi:10.1086/165094.

[Nauenberg(2008)] Nauenberg, M., "Edmund C. Stoner and the Discovery of the Maximum Mass of White Dwarfs", Journal for the History of Astronomy, vol. 39, pp. 297–312, 2008. doi:10.1177/002182860803900302.

[Neyman and Pearson(1928)] Neyman J, Pearson ES: On the Use and Interpretation of Certain Test Criteria for Purposes of Statistical Inference: Part I. Biometrika. 1928;20A(1/2):175–240. 10.3389/fpsyg.2015.00245

[Patterson et al.(1981)] Patterson, J., "Rapid oscillations in cataclysmic variables. VI. Periodicities in erupting dwarf novae.", The Astrophysical Journal Supplement Series, vol. 45, pp. 517–539, 1981. doi:10.1086/190723.

[Piro et al.(2014)] Piro, A. L. and Thompson, T. A., "The Signature of Single-degenerate Accretion-induced Collapse", The Astrophysical Journal, vol. 794, no. 1, 2014. doi:10.1088/0004-637X/794/1/28.

[Pringle & Rees(1973)] Pringle, J. E. and Rees, M. J., "On the Optical Behaviour of Binary X-ray Sources.", vol. 5, p. 42, 1973.

[Qian et al.(2012)] Qian, S.-B., Liu, L., Zhu, L.-Y., Dai, Z.-B., Fernández Lajús, E., and Baume, G. L., "A circumbinary planet in orbit around the short-period white dwarf eclipsing binary RR Cae", Monthly Notices of the Royal Astronomical Society, vol. 422, no. 1, pp. L24–L27, 2012. doi:10.1111/j.1745-3933.2012.01228.x.

[Ramsay et al.(2018)] Ramsay, G., "Physical properties of AM CVn stars: New insights from Gaia DR2", Astronomy and Astrophysics, vol. 620, 2018. doi:10.1051/0004-6361/201834261.

[Ramsay et al.(2019)] Ramsay, G., Kennedy, M., Hakala, P., and Jeffery, C. S., "Spectroscopic observations of AM CVn binary candidates MGAB-248 and MGAB-249", ATel13048, 2019.

[Rau et al.(2009)] Rau, A., "Exploring the Optical Transient Sky with the Palomar Transient Factory", Publications of the Astronomical Society of the Pacific, vol. 121, no. 886, p. 1334, 2009. doi:10.1086/605911.

[Remillard et al.(1991)] Remillard, R. A., Stroozas, B. A., Tapia, S., and Silber, A., "The Eclipsing AM Herculis Variable H1907+690", The Astrophysical Journal, vol. 379, p. 715, 1991. doi:10.1086/170546.

[Richer et al.(1997)] Richer, H. B., "White Dwarfs in Globular Clusters: Hubble Space Telescope Observations of M4", The Astrophysical Journal, vol. 484, no. 2, pp. 741–760, 1997. doi:10.1086/304379.

[Rivera et al.(2019)] Rivera Sandoval, L. E., Maccarone, T., and Murawski, G., "Swift observations of two new AM CVn candidates", ATel12847, 2019.

[Rixon et al.(2014)] Rixon, G., "Gaia Alerts classified at the William Herschel Telescope", ATel.6593, 2014.

[Scargle(1981)] Scargle, J. D. "Studies in Astronomical Time Series Analysis. I - Modeling Random Processes in the Time Domain." The Astrophysical Journal Supplement Series, vol. 45, Jan. 1981, p. 1., https://doi.org/10.1086/190706.

[Scargle(1982)] Scargle, J. D. "Studies in Astronomical Time Series Analysis. II - Statistical Aspects of Spectral Analysis of Unevenly Spaced Data." The Astrophysical Journal, vol. 263, Dec. 1982, p. 835., https://doi.org/10.1086/160554.

[Scargle (1989b)] Scargle, J. D., "An introduction to chaotic and random time series analysis", International Journal of Imaging Systems Technology, vol. 1, pp. 243–253, 1989.

[Scargle(1989)] Scargle, J. D. "Studies in Astronomical Time Series Analysis. III - Fourier Transforms, Autocorrelation Functions, and Cross-Correlation Functions of Unevenly Spaced Data." The Astrophysical Journal, vol. 343, Aug. 1989, p. 874., https://doi.org/10.1086/167757.

[Scargle(1990)] Scargle, J. D. "Studies in Astronomical Time Series Analysis. IV - Modeling Chaotic and Random Processes with Linear Filters." The Astrophysical Journal, vol. 359, Aug. 1990, p. 469., https://doi.org/10.1086/169079.

[Scargle(1998)] Scargle, J. D. "Studies in Astronomical Time Series Analysis. V. Bayesian Blocks, a New Method to Analyze Structure in Photon Counting Data." The Astrophysical Journal, vol. 504, no. 1, Sept. 1998, pp. 405–18., https://doi.org/10.1086/306064.

[Scargle(2002)] Scargle, Jeffrey D. "Bayesian Estimation of Time Series Lags and Structure." AIP Conference Proceedings, vol. 617, AIP, 2002, pp. 23–35., https://doi.org/10.1063/1.1477036.

[Schuster(1898)] Schuster, Arthur. "On the Investigation of Hidden Periodicities with Application to a Supposed 26 Day Period of Meteorological Phenomena." Journal of Geophysical Research, vol. 3, no. 1, 1898, p. 13., https://doi.org/10.1029/TM003i001p00013.

[Schwab et al.(2015)] Schwab, J., Quataert, E., and Bildsten, L., "Thermal runaway during the evolution of ONeMg cores towards accretion-induced collapse", Monthly Notices of the Royal Astronomical Society, vol. 453, no. 2, pp. 1910–1927, 2015. doi:10.1093/mnras/stv1804.

[Schwarzenberg-Czerny(1989)] Schwarzenberg-Czerny, A. 1989, Monthly Notices of the Royal Astronomical Society, 241, 153. doi:10.1093/mnras/241.2.153

[Schwarzenberg-Czerny(1996)] Schwarzenberg-Czerny, A. "Fast and Statistically Optimal Period Search in Uneven Sampled Observations." The Astrophysical Journal, vol. 460, no. 2, Apr. 1996., https://doi.org/10.1086/309985.

[Schwarzenberg-Czerny(1997)] Schwarzenberg-Czerny, A. "The Correct Probability Distribution for the Phase Dispersion Minimization Periodogram." The Astrophysical Journal, vol. 489, no. 2, Nov. 1997, pp. 941–45., https://doi.org/10.1086/304832.

[Shannon(1948)] Shannon, C. E. "A Mathematical Theory of Communication." Bell System Technical Journal, vol. 27, no. 3, July 1948, pp. 379–423. DOI.org (Crossref), https://doi.org/10.1002/j.1538-7305.1948.tb01338.x.

[Shears et al.(2011)] Shears, J., "The orbital and superhump periods of the deeply eclipsing dwarf nova SDSS J150240.98+333423.9", Journal of the British Astronomical Association, vol. 121, pp. 96–104, 2011.

[Southworth et al.(2015)] Southworth, J., Tappert, C., Gänsicke, B. T., and Copperwheat, C. M., "Orbital periods of cataclysmic variables identified by the SDSS. IX. NTT photometry of eight eclipsing and three magnetic systems", Astronomy and Astrophysics, vol. 573, 2015. doi:10.1051/0004-6361/201425060.

[Stellingwerf(1978)] Stellingwerf, R. F. "Period Determination Using Phase Dispersion Minimization." The Astrophysical Journal, vol. 224, Sept. 1978, p. 953., https://doi.org/10.1086/156444.

[Stoner(1929)] Stoner, E. C.(1929). V.The limiting density in white dwarf stars. The London, Edinburgh, and Dublin Philosophical Magazine and Journal of Science, 7(41), 63–70. doi:10.1080/14786440108564713

[Stoner(1930)] Stoner, E., "The Equilibrium of Dense Stars", The London, vol. 9, no. 60, pp. 944–963, 1930.

[Szkody et al.(2006)] Szkody, P., "Cataclysmic Variables from Sloan Digital Sky Survey. V. The Fifth Year (2004)", The Astronomical Journal, vol. 131, no. 2, pp. 973–983, 2006. doi:10.1086/499308

[Szkody et al.(2009)] Szkody, P., "Cataclysmic Variables from SDSS. VII. The Seventh Year (2006)", The Astronomical Journal, vol. 137, no. 4, pp. 4011–4019, 2009. doi:10.1088/0004-6256/137/4/4011.

[Thorne et al.(2010)] Thorne, K., Garnavich, P., and Mohrig, K., "The Polar CSS 081231:071126+440405 at a Low Accretion Rate", Information Bulletin on Variable Stars, vol. 5923, p. 1, 2010. doi:10.48550/arXiv.1002.0339.

[Vanderplas(2018)] VanderPlas, Jacob T. "Understanding the Lomb–Scargle Periodogram." The Astrophysical Journal Supplement Series, vol. 236, no. 1, May 2018, p. 16., https://doi.org/10.3847/1538-4365/aab766.

[Vaníček(1969)] Vaníček, Petr. "Approximate Spectral Analysis by Least-Squares Fit: Successive Spectral Analysis." Astrophysics and Space Science, vol. 4, no. 4, Aug. 1969, pp. 387–91., https://doi.org/10.1007/BF00651344.

[Vio et al.(2013)] Vio, R., et al. "Irregular Time Series in Astronomy and the Use of the Lomb–Scargle Periodogram." Astronomy and Computing, vol. 1, Feb. 2013, pp. 5–16., https://doi.org/10.1016/j.ascom.2012.12.001.

[Vityazev(1996)] Vityazev, V. V. "Time Series Analysis of Unequally Spaced Data: The Statistical Properties of the Schuster Periodogram and LS-Spectra." Astronomical & Astrophysical Transactions, vol. 11, no. 2, Nov. 1996, pp. 159–73., https://doi.org/10.1080/10556799608205462.

[Vogel et al.(2008)] Vogel, J., Byckling, K., Schwope, A., Osborne, J. P., Schwarz, R., and Watson, M. G., "The serendipituous discovery of a short-period eclipsing polar in 2XMMp", Astronomy and Astrophysics, vol. 485, no. 3, pp. 787–795, 2008. doi:10.1051/0004-6361:20079341.

[Wright(1935)] Wright, W. H. "Comments on Nova Herculis 1934." Publications of the Astronomical Society of the Pacific, vol. 47, no. 275, 1935, pp. 47–49. JSTOR, http://www.jstor.org/stable/40670634.